Proceedings of International Conference
Applications of Structural Fire Engineering
Prague, 19-20 February 2009

Session 2

Fire Modelling

FIRE SCENARIO AND STRUCTURAL BEHAVIOUR OF UNDERGROUND PARKING LOTS EXPOSED TO FIRE

Patrick Bamonte, Roberto Felicetti

Department of Structural Engineering, Politecnico di Milano, Milan, Italy

INTRODUCTION

The increasing diffusion of underground parking lots, mainly in congested urban areas, makes the fire safety of these structures a real challenge during the entire design process. As a matter of fact, (a) the reduced extension of the in-plan areas puts strict limits on the evacuation paths, that require an accurate design, and (b) the rather low ceiling and lack of openings can significantly influence both the fire scenario and the ensuing thermal field, making it imperative to study each single case, without relying on the usual standard fire curves. As a consequence, the resulting temperatures can be higher than in typical buildings and the structural members can be more severely damaged than in usual cases.

All these factors, and especially the exposure to unusual fire scenarios, makes prescriptive design hardly applicable and performance-based design a must, from the identification of the most appropriate temperature-time curve, to the evaluation of the bearing capacity of each structural member. This phase is crucial, since parking lots are often built with rather thin structural members, such as prestressed open-section or double-tee beams and slabs. In the former case, for example, the pre-tensioned reinforcement is very close to the heated surface, and thus prone to thermally-induced mechanical decay, to the detriment of the overall bearing capacity. In the latter case, the thermal damage in concrete outer layers may significantly reduce the structural ductility, in so favouring brittle phenomena like – for instance – punching-shear failures.

The objective of this paper is to investigate the main factors governing the fire behaviour of a typical underground parking lot consisting of a flat slab supported by a number of relatively slender columns. On the basis of the available literature [1] and of reasonable assumptions, the fire scenario is worked out firstly, by properly modelling the heat transfer between the ambient and the structural members. This preliminary step is instrumental in determining the temperature-time curve required by the thermal analysis of the structural members. On the basis of the calculated thermal field, it is possible to evaluate the decay of the mechanical properties (strength and stiffness) as a function of the temperature [2]. The strength decay results in a general reduction of the bearing capacity, that can be studied by means of well-established simplified methods. The stiffness decay, together with the thermal deformations, often brings in significant redistributions of the internal forces [3,4]. The main factors – and especially the role played by materials' nonlinearity – are studied and some general considerations are drawn on the overall safety of the structure under examination.

1 GEOMETRY AND MATERIALS

The structure considered in the following is a rectangular flat slab resting on square columns and on four perimeter walls (Fig. 1). The two rows of columns divide the slab in a main span (= 8.00 m), and two minor lateral spans (= 4.50 m): thus, there is a central lane for the car movement, and two side aisles for car parking. For the sake of simplicity, the spans comprised between adjacent columns and the columns themselves have been numbered (spans = C1-C15; columns = P1-P8).

The thickness of the slab is assumed to be 35 cm, thus yielding a structural slenderness of ≈ 23, which is a reasonable value for these kind of structures. The structure is made of normal-strength concrete (f_{ck} = 25 MPa, E_c = 31000 MPa, ν = 0.16), and reinforced with ordinary steel (E_s = 200000 MPa, f_y = 500 MPa).
The external loads consist only of the soil, which is assumed to be about 1 m deep. Therefore, the distributed load per unit area is assumed to be 30 kN/m^2 (self-weight ≈ 9.00 kN/m^2; permanent loads ≈ 21 kN/m^2, corresponding to ≈ 1.20 m of ground above the slab).

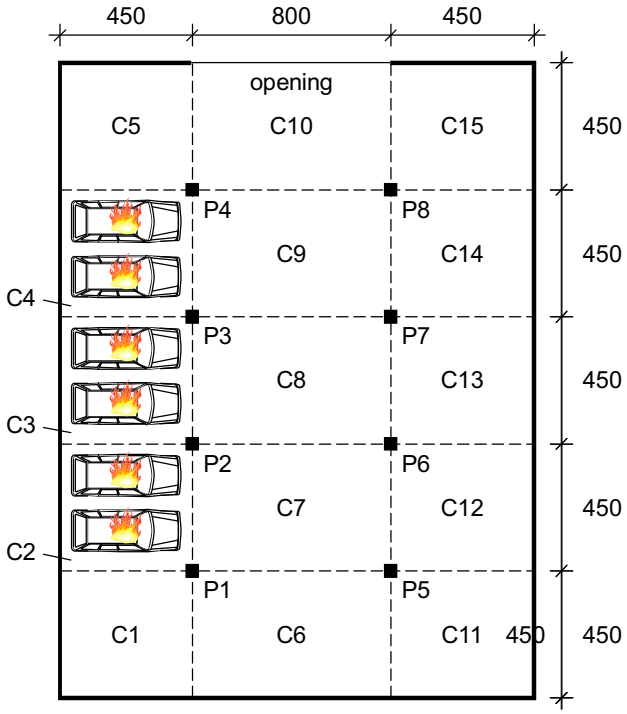

Fig. 1. Plan view of the structure considered

2 FIRE SCENARIO

The fire event considered is due to the ignition of six cars in the left aisle of the parking lot. It is assumed that the fire starts at the car near column P1, and then propagates to the nearby cars. Each car takes fire approximately 15 minutes after the previous one; the resulting fire duration is close to 120 minutes.
The number of cars involved in the fire implies that almost the whole left aisle will be subjected to fire. However, the resulting fire remains localized, and the condition for flash-over to occur is not reached. The evolution of the temperature inside the compartment could be evaluated properly only by means of a CFD calculation; this would be rather time-consuming, and CFD calculations are not suited to be performed easily by a structural engineer, especially in the design phase. As an alternative, the EN 1991-1-2 allows the use of simplified models, such as one- and two-zone models, which are based on simplified balance equations between the different heat contributions involved in the fire event inside a given compartment.

Two-zone models have been implemented in several free-downloadable softwares: in our case, reference was made to OZone (developed at the University of Liège, Belgium) and CFAST (developed at NIST, USA).
Both softwares require the input of the fire scenario in terms of HRR (Heat Release Rate) curve. In the present case, the evaluation of the power developed by the burning of one single car was performed in accordance to the experiments carried out by Li and Spearpoint [1] on different means of transportation. The HRR curve measured during the ignition of a normal-size car (Austin Maestro) was used in the following (Fig. 2a).
In the case of CFAST, the single curve can be used as input for the calculation: the different cars igniting are then represented as single fires, characterized by the same HRR curve, but different starting and location points (in space and time). In the case of OZone, the total HRR needs to be input: therefore, the total HRR was evaluated as the sum of the six HRR-curves properly delayed in time, and input into the software. The result is shown in Fig. 2b: the continuous line represents the input, the dashed line represents the input computed by the software (which represents a sort of average of the real input curve).

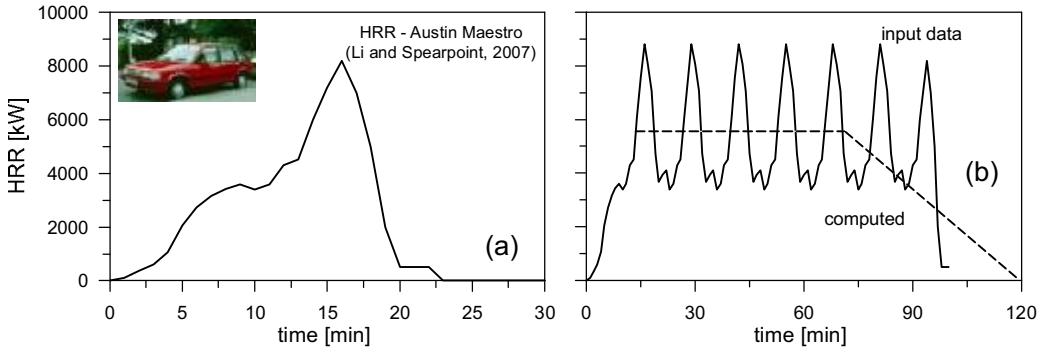

Fig. 2. (a) HRR measured from a car fire experiment [1]; (b) total HRR, calculated as the sum of the curves of 6 cars igniting (each car is assumed to start burning approximately 15 minutes after the previous one)

The resulting temperatures of the "hot layer" as a function of time (as evaluated by means of the two softwares) are depicted in Fig. 3a. It is worth noting that the temperature-time curve computed by OZone is smoother (probably because of the smoother input curve); moreover, the temperature-time curves evaluated by means of the two softwares, are in very good agreement.
The most crude approximation of these calculations is the assumption that the whole compartment of the parking lot behaves as a unique ambient (although subdivided into a hot and a cold layer), and thus the evaluation of a unique temperature-time curve. A possible refinement is to divide the lot into 15 compartments (C1-C15, see Fig. 1); this subdivision is only virtual, since no partitions are placed between adjacent compartments. This circumstance was incorporated in CFAST, by introducing 15 different compartments with great openings as partitions. In this case, the thermal input is implemented by placing the burning cars (each described by the single HRR curve in Fig. 2a) in compartments C2, C3 and C4. By working out the temperatures in the "virtual" compartments C1-C15, the evolution of temperature in space (and not only in time) can be assessed.
The resulting temperatures in the hottest compartments (C1-C5) are shown in Fig. 3b: the trends are rather serrate, probably because of the sharp shape of the input HRR curve

(Fig. 2a). Comparing the results with the curves obtained under the assumption of one single compartment (Fig. 3a), it is worth noting that the maximum temperatures are significantly higher. There are also sizable differences between the different compartments: for example, T1 is approximately half of T4, at least beyond 30 minutes from the beginning of the fire.

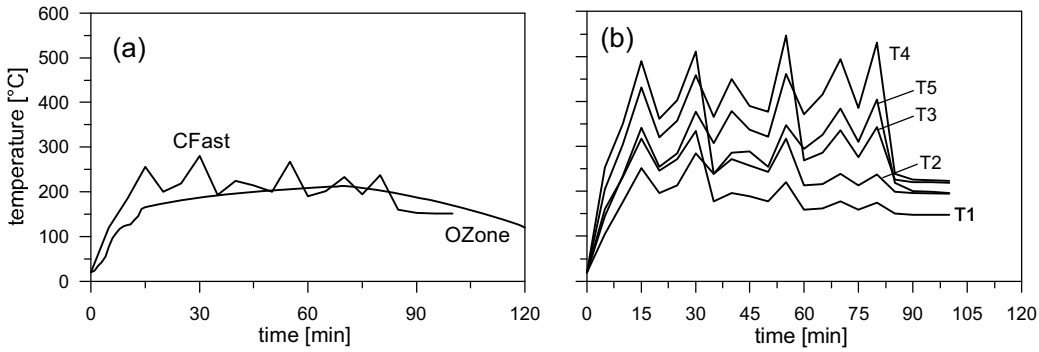

Fig. 3. (a) Temperature-time curves, calculated by the two codes used under the assumption of a single compartment; (b) temperature-time curves for the compartments on the left aisle (as evaluated with CFAST).

3 FINITE ELEMENT MODEL

The structural behaviour was studied by means of a finite elements model. The slab was modelled by means of plate elements, allowing for a sequentially-coupled thermo-mechanical behaviour (i.e. the temperature affects the stress and displacement variables, but not vice versa). Different analyses were carried out, under different assumptions concerning the thermal input, the boundary restraints and, above all, the geometrical and materials' non-linearity. The different assumptions were implemented individually, in order to better highlight their specific effect on the overall behaviour.

A first set of analyses was carried out under the assumption that the behaviour of the material be elastic and temperature-independent. Therefore, since cracking of the concrete is not explicitly introduced, the reinforcement needs not be considered.

In the first analysis (A1) the boundary walls and columns are modelled as simple supports (i.e. the confining effect of the soil, as well as the bending stiffness of the walls and columns, are neglected). The thermal input consists of the temperature-time curves shown in Fig. 3b for the left compartments, together with the other curves (not plotted in Fig. 3b) for the remaining 10 compartments. The thermal flux entering the heated surface of the slab is determined by convection (convection coefficient = 35 W/[m^{2}K], see EN 1991-1-2), and radiation (emissivity of the heated surface = 0.8, see EN 1991-1-2).

The resulting axial loads on the columns as a function of time are shown in Fig. 4a: the most significant increase in the axial load (N^{fire}/N^{20} = 2.5÷4.0) occurs in the columns belonging to the left aisle of the parking lot (P1-P4, see Fig. 1), as should have been expected, since they are closer to the localized fires. The axial load on the remaining columns exhibits either a minor increase (P5 and P8, N^{fire}/N^{20} = 1.5), or remains practically constant (P6 and P7). It is worth noting that the sequence of the peaks of the axial loads in columns P1-P4 as a function of time is closely related to the sequence of the 6 cars igniting (from C2 to C4), with P1 being the first column to reach the peak of the axial load, and P4 the last: therefore, the 6 burning cars generate a sort of "heat wave" propagating from C2 towards C4. A possible consequence

is the fact that the column characterized by the highest peak in the axial load is P4, with a peak of the compression force during the fire almost 4 times the value at ambient temperature. The sensitivity of the structure to the various factors (thermal input, confining effect of the soil, boundary restraints) coming into play has been ascertained by means of a set of three more numerical analyses. More in detail:

- A2: the temperature-time curve is the same for all spans (i.e. the variability of the temperature with space is neglected), and equal to the smooth curve of Fig. 3a (determined by means of OZone);
- A3: the boundaries are modelled as perfect in-plane restraints for the slab, and the second-order effects (= geometrical non-linearity) are taken into account;
- A4: the boundaries of the slab are considered to be built in.

The comparison between the various analyses was carried out with reference to column P4, that exhibits in all cases the largest increase of the axial load.

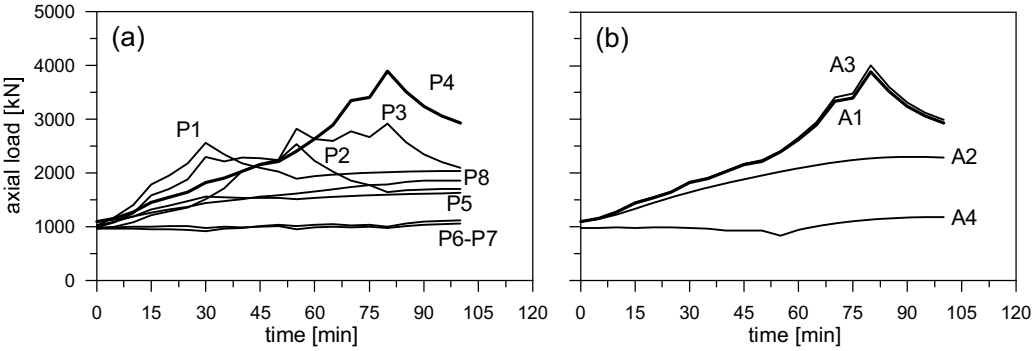

Fig. 4. (a) Axial loads in columns P1-P8 as a function of time; (b) axial load in column P4 for different assumptions concerning thermal input, boundary restraints and 2nd order effects.

The comparison between curves A1 and A2 shows that the effect of a non-uniform heating is detrimental, probably because different values of the thermal curvature in adjacent spans tend to increase the shear force at the interface; this increase results in a higher axial load on the columns. Consequently, a uniform heating leads to a lower increase of the axial load during the fire.
As for the 2nd-order effects due to the confining effect of the boundaries (A3), they seem to play a minor role, most probably because the displacements reached during the fire are limited by the presence of the columns: as a matter of fact, membrane effects are significant for slab structures characterized by larger slenderness (and thus large displacements in fire). Finally, if the slab has built-in edges (A4), the axial load is hardly affected by the fire.
Two further analyses were then performed, to account for the decay of the elastic modulus with temperature (evaluated in accordance to the provisions given in EN 1992-1-2); the thermal inputs were the same as in the case of A1 and A2. The comparison was carried out in terms of axial load on column P4, and the results are shown in Fig. 5.
If the dependence on temperature of the elastic modulus of concrete is taken into account, both in the case of non-uniform (dashed curve) and uniform heating (dash-dotted curve), the resulting axial load on column P4 is significantly lower than in the corresponding reference cases (A1 and A2 respectively); however, the value is still 50% higher than at room temperature.

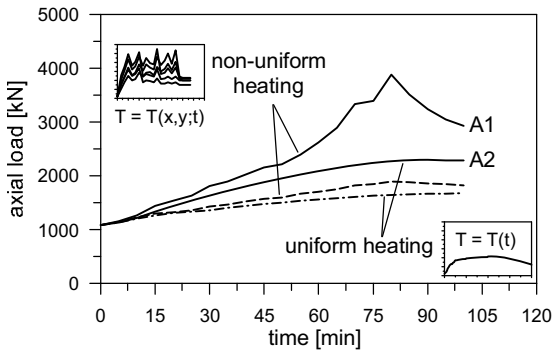

Fig. 5. Axial load on column P4 as a function of time, assuming a constant elastic modulus (A1 = non-uniform heating and A2 = uniform heating), or taking into account its reduction with temperature (dashed and dash-dotted curve respectively).

4 CONCLUDING REMARKS

The thickness of thin flat slabs supported by columns is usually designed by limiting the displacements under the service loads, and by ensuring a satisfying level of safety against punching shear at ultimate. In the case of the roof of a parking lot subjected to the fire of a limited number of cars, a generalized increase of the axial load on the columns is to be expected. This increase becomes even more significant, if the localized nature of car fires is taken into account, and properly introduced by considering the dependence of ambient temperature not only from time, but also from space. The differences ensuing from the distribution of temperature in space (non-uniform heating vs. uniform heating) tend to vanish, if the reduction of the elastic modulus with temperature is taken into account; the same would probably be observed, if concrete cracking and rebar yielding were considered. However, the axial load can still exhibit an increase of up to 50% with respect to its value at 20°C, making these structures very sensitive to punching shear failures triggered by fire.

5 ACKNOWLEDGMENTS

The authors are grateful to Prof. Pietro Gambarova for his valuable suggestions. The contribution of Antonio Buccinnà in the numerical simulations concerning the fire scenario is also gratefully acknowledged.

REFERENCES

[1] Y. Li and M. Spearpoint (2007): "Analysis of Vehicle Fire Statistics in New Zealand Parking Buildings", *Fire Technology*, 43, pp. 93–106.

[2] G.A. Khoury (2000): "Effect of Fire on Concrete and Concrete Structures", *Progress in Structural Engineering Materials*, 2000, 2, pp. 429-447.

[3] F. Biondini and A. Nero (2006): "Nonlinear Analysis of Concrete Structures under Fire", 2nd *fib* Congress, Paper 12-5, Naples, June 5-8, 2006.

[4] P. Riva and J.-M. Franssen (2008): "Structural Behavior of Continuous Beams and Frames", Chapter 4 in *fib* Bulletin 46 "Fire design of concrete structures – structural behavior and assessment", 210 pp.

DEFINITION AND SELECTION OF DESIGN FIRE SCENARIOS

Konstantinos Gkoumas, Chiara Crosti, Luisa Giuliani, Franco Bontempi

University of Rome "La Sapienza", School of Engineering, Rome, Italy

INTRODUCTION

The problem of structural fire safety in the recent years has gained a predominant role in the engineering design. This is because nowadays, always bigger and more complex structures are designed and build, making use of particularly fire sensitive materials such as steel, and also, because there is an increasing belief that structures not only have to resist to the design loads, but to maintain a minimal performance in accidental situations as well. The necessity to pursue these goals, has led to the growth of the branch of Fire Safety Engineering, especially after the 9-11 events, which led to the WTC tower collapses in the United States.
Although at present there is no internationally agreed definition of Fire Safety Engineering (FSE), it can be defined as the application of engineering principles, rules and expert judgement based on a scientific understanding of the fire phenomena, of the effects of fire and of the reaction and behaviour of people, in order to:

- save life, protect property and preserve the environment and heritage;
- quantify the hazards and risk of fire and its effects;
- evaluate analytically the optimum protective and preventative measures necessary to limit, within prescribed levels, the consequences of fire.

In a FSE complying strategy, a number of objectives is identified (safety of life, conservation of property, continuity of business operations, preservation of heritage, etc.). These (qualitative) objectives, must be characterised by setting specific performance criteria. Regarding in particular safety of life, the principal aim is to ensure the necessary time for the safe evacuation. In [1] NIST recommends a number of measures, starting from "hard" measures related to building performance factors, such as the checking of the structural integrity and the endurance under fire, and extending to issues related to the human performance, such as the evacuation measurements, training of the personnel etc.
Regarding in particular the performance of the structure under fire, performances can be assessed with the implementation of analytical and computational tools, tools which require a very good understanding of the fire phenomenon. In a second paper presented at the same conference [2], some fundamental considerations regarding the structural safety of steel structures, are presented, as a practical exemplification of many of these concepts.
From what said above, the performance evaluation of the structure becomes important. In this perspective, within the approach assumed in a FSE complying context, two single concepts have found application (the second one, also as a complement to the other):

- The Performance Based Fire Safety Design (PBFSD) of the structure;
- The Fire Risk Assessment (FRA) of the structure.

With aid from the above concepts it is possible to define and select design fire scenarios, leading to the identification of design fires implemented within finite element analysis, in order to inquire on the requested performances.

1 PERFORMANCE BASED FIRE SAFETY DESIGN

Performance Based Design (PBD) in general, is the design that meets a specified performance level rather than prescribe specific design criteria (see for example [3]). Performance Based Fire Safety Design (PBFSD) is a new concept within Fire Safety engineering, and it is based on the premises of PBD.
PBFSD allows the use of any design that demonstrates compliance with the fire safety goals of the code. Fire safety goals commonly addressed include life safety, property protection, continuity of operations, and environmental protection. These fire safety goals are explicitly stated in the code, as are the methods that can be used to demonstrate compliance.
A PBFSD starts with an analysis of fire scenarios to determine which design alternatives will meet those fire safety goals. These goals are either referred to the structural performance or to the performance of the system in general. In the first case, the focus is on the structural performance in the presence of fire and includes requirements of fire resistance for the structural elements (e.g. beams, slabs, columns) or for the structural system as a whole (avoidance of excessive vibrations, avoidance of progressive collapse, etc.). In the second case, the focus is on the general design for safety in the case of fire, dealing mostly with the evacuation provisions, at conditions extended well before an eventual structural failure or collapse. In both cases the final goal is the same: the minimization of the consequences to the public. This is in generally attained by assuring a minimum performance (both structural and operational) for the evacuation time.
The PBFSD becomes important especially in the case of complex structural systems or unique buildings, for which a prescriptive approach is difficult to apply for several reason, among else, aesthetics.

1.1 Performance Based Structural Design for Fire Safety

The performance approach for the structural design of structures begun to diffuse in the last sixty years, mostly for facilities with elevated risk of fire. This kind of Performance Based approach, has been applied in other circumstances, particularly for seismic design.
The focus is on the structural performance in the presence of fire and includes requirements of fire resistance for the structural elements (e.g. beams, slabs, columns) or for the structural system as a whole (avoidance of excessive vibrations, of progressive collapse, etc.). A very important step to guarantee a determinate level of safety is to verify that the resistance of the structure under fire is higher than the fire severity (fire resistance > fire severity). There are three techniques of checking for the fire resistance (in the time, temperature or resistance domain), as explained among else in the Italian Building Code [4], as shown in *Table 1*.

Table 1. Fire resistant checks (from [4])

Domain	Units	Fire resistance	Fire severity
Time	Hours	Time over that the structure is weakened	Duration of fire
Temperature	ºC	Temperature over that the structure is weakened	Maximum temperature reached during fire
Resistance	KN or KNm	Load bearing capacity at high temperature	Applied load during fire

Generally, when assessing the performance of a structure subject to fire, a conventional collapse is defined, related to the typology of structural element and to the function that it must accomplish. For additional details, the reader is referred to [2] presented at the same conference.

1.2 Performance Based Design for Fire Safety - human performance/system response

The principal issue again is the evacuation of a building. The evacuation time is strongly related to some characteristics related to the building geometry and inner organization (e.g. the number of emergency doors per floor, the door dimensions, the maximum travel distance to the exit). While in a prescriptive code, specific data are given, on the basis of the building usage, a performance based code, investigates on how to achieve the same goal as of the numerical prescriptive requirements.
As an example [5] indicates a number of PBD indications, that could substitute specific numerical prescriptive requirements of a prescriptive code:

- provide a maximum travel distance over which safe conditions for egress;
- provide a sufficient number of exits from an area of generally high density occupant load to allow for safe egress;
- provide a sufficient number of exits from a floor area where the large number of people need more than two exits from the area in the event of an evacuation (instead of providing a specific number of exits).

2 DESIGN FIRE SCENARIOS AND DESIGN FIRES

For the appropriate fire performance assessment of the structure, fire scenarios have to be identified, with the consequent selection of design fire scenarios, and finally, of the design fires.
In the process of selecting a design fire, several phases have to be identified. These are documented in many International codes and standards (see for example [6,7]). In *Fig. 1*, a schematic flowchart is presented, closely based on indication provided in [7], in which the various phases leading to the selection of design fires are described.

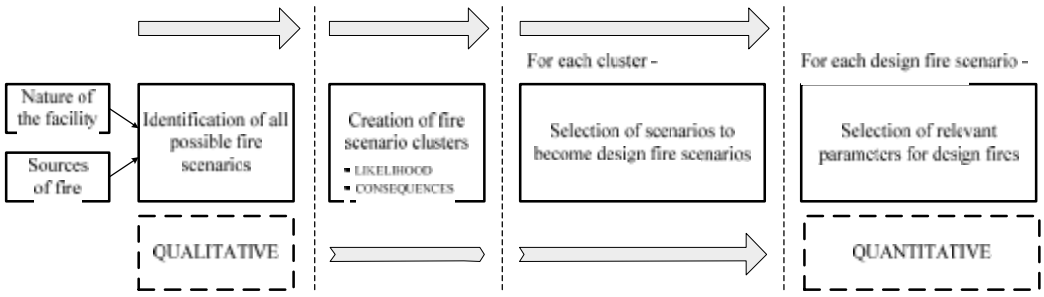

Fig. 1. Selection of design fires

With reference to the above flowchart, in a first place, all apparently possible fire scenarios are identified on the basis of the nature of the facility and the possible sources of fire. This leads to the identification of a vast number of -qualitatively described- possible fire scenarios. These scenarios have to be "filtered" and categorised in cluster of scenarios. For each cluster, a risk is associated characterised in terms of the likelihood of occurrence of the cluster and the resultant consequence. The estimated risk can be either qualitative or quantitative (depending on the risk analysis performed and the necessity on a case by case basis). From each cluster of scenarios, those candidate to became design fires are selected. The selection can be based on different processes, ranging from pure judgement to risk analysis techniques such as risk ranking or the construction of event trees. Some additional considerations regarding the fire risk assessment of a structure are given in paragraph 3, while a practical exemplification of

the construction of event trees is presented in paragraph 4. Finally, for each fire scenario selected, a design fire scenario is obtained on the basis of a ranking process.
From the obtained design fire scenarios, one or more design fires are obtained, characterised by quantified data, specific for a given fire safety design objective. Briefly stated, a design fire is characterized by quantities such as its heat release rate at any moment in time, its growth rate, the combustion product rate (such as smoke particulate, toxic or corrosive species, etc.) and the production rate [6]. In the process of selecting the design fire, burning rate data on actual materials should be used. A broadly accepted way to classify design fires is in function the heat release rate: in [7] design fires are classified as slow, medium, fast and ultra fast fires. Other ways to classify a design fire are proposed in literature, e.g. by default curves as a function of the type of the building (see for example [8]).

3 FIRE RISK ASSESSMENT OF THE STRUCTURE

The Fire Risk Assessment (FRA) of the structure, is an incorporated part of the PBFSD, and is codified in many Standards [5,9-11]. One of the aims of the Standards is to provide the methodology on how to evaluate the scenarios to be considered for further analysis, by means of standard methods of Risk Analysis (e.g. qualitative, quantitative, probabilistic etc.).
In particular, within a Risk Management Process, system hazards, their contributing factors and possible sources, must be identified, analyzed and ranked. In particular, any object that emits sufficient heat to ignite combustibles, based on proximity and ignitability, constitutes an initiating hazard, having potential to initiate an unwanted fire. In the first place, the use of a Preliminary Hazards Analysis (PHA) method is suitable. This method includes the ranking of hazards by severity and probability, the inquiry of operational constraints and a list of recommended actions to eliminate or control the hazards. The advantage of a PHA approach is that an inventory of possible hazards can be easily generated. On the downside, some hazards can be missed, thus it is not easy to have an insight into overall risk associated with the system. More systematic and detailed methods to System Hazards Identification include Hazard and operability study (HAZOP) and Failure modes and effects analysis (FMEA). The first is a method of group examination to identify hazards and their consequences, while the latter identifies the modes in which each element can fail and determines the effect on the system. The reader is referred to specialized texts for additional details.

4 DEFINITION OF DESIGN FIRE SCENARIOS FOR A STRUCTURAL SYSTEM

The previous exposed theoretical arguments, find a practical exemplification in the Fire Risk Assessment of a complex structural system, exposed in detail in [12]. The object under inquiry is an industrial facility in steel frame, used for the storage and maintenance of helicopters.
Due to the particular usage, this facility presents an elevated fire risk. The structure is 64.64 meters long, 32.85 meters wide and has a maximum height of 12.9 meters. The triggering event consider is the fire ignition on a helicopter.
The choice of important fire scenarios for the case studied is focused on three areas that, after an initial evaluation, seem to produce the most adverse fire scenarios (in the sense of "likelihood *times* consequence").
The identified most severe areas for the starting of the fire give birth to a number of scenarios, localized in zone of about 50 m^2, that accounts for about the 2,5% of all the building surface.
The fire risk prone areas identified are three (*Fig. 2*):

1. The central zone of the building (Area A).
2. The central zone of the span (Area B).
3. The outer zone (Area C).

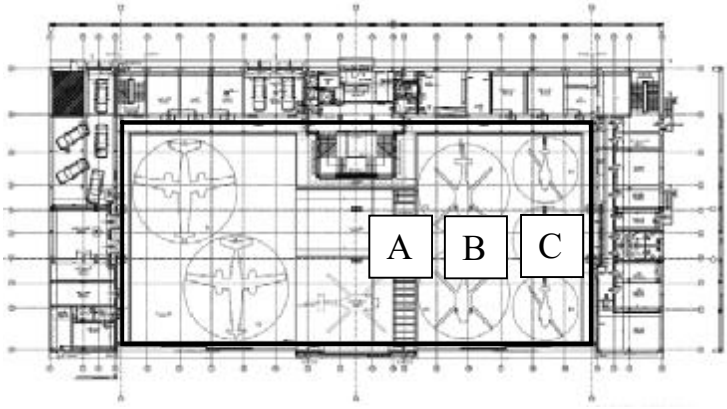

Fig. 2. Plan of the industrial facility

The event tree representing the evolution of a generic triggering event is further divided to take account for more than one initial situations. The one presented here, is relevant to a condition where the doors of the facility are closed, however, there are employees inside.
In the event tree of *Fig. 3*, the consequences of an initiative event are followed in a series of possible paths.

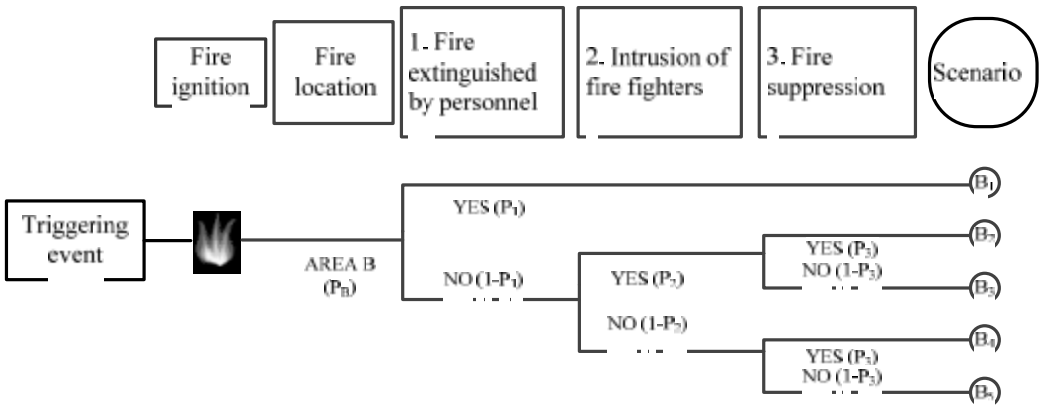

Fig. 3. Event tree after a fire ignition in the industrial facility

The analysis can be quantified by assigning numerical values to the probabilities (e.g. making use of appropriate historical values) as shown for example in *Table 2* in the case of a triggering event in area B.

Table 2. Probabilities for the occurrence of different scenarios

Scenario	Probability
B_1	P_B*P_1
B_2	$P_B*(1-P_1)*P_2$
B_3	$P_B*(1-P_1)*(1-P_2)*P_3*P_4$
B_4	$P_B*(1-P_1)*(1-P_2)*P_3*(1-P_4)$
B_5	$P_B*(1-P_1)*(1-P_2)*(1-P_3)*P_4$
B_6	$P_B*(1-P_1)*(1-P_2)*(1-P_3)*(1-P_4)$

The indicated probabilities are intended as in function of time, that is, P = P (t). In this sense, P_4 is not the same after condition 3 (intrusion of the fire fighters), since the expansion of the fire is different for the two cases. For the same reason, probabilities of the various branches are different for the 3 different areas (e.g. the probability P_2 of the fire being extinguished by the sprinklers, is different for each one of the Areas, since the sprinkler arrangement is different in each area). The same stands for probabilities assigned for the different fire locations (not shown here for the sake of brevity), due to the different geometric characteristics and the different internal configuration of each area.

5 FURTHER CONSIDERATIONS

The aspects covered in this paper show that only with a faithful representation of the system, a truthful definition of fire scenarios and, as will be shown, detailed advanced analysis, it is possible to have a clear view on the consequences of a fire. Design fire scenarios identified and selected in this paper, led to the implementation of design fires in FEM (as shown in the 2nd application in [2] presented at the same conference), aiming at the assessment of specific structural performances, in particular the collapse resistance of the structure. Although the process of defining design fire scenarios is complex and characterised by uncertainties, the authors believe that with scrupulous applications of engineering principles that have found ground in the recent years, and the necessary engineering judgement, it is possibly to realistically depict the phenomena in the civil engineering field.

REFERENCES

[1] NIST NCSTAR 1, WTC Investigation, Chapter 9, Recommendations. Available online on 01/2008 at http://wtc.nist.gov/NCSTAR1

[2] Crosti, C., Giuliani, L., Gkoumas, K., Bontempi, F., Structural analysis of steel structures under fire loading, Book Proceedings: Applications of Structural Fire Engineering, Prague 19-20 February 2009.

[3] Foliente, G., Developments in Performance-Based Building Codes and Standards, Forest Products Journal., Vol.50, No 7/8, 2000.

[4] D.M. 14/09/2005- Norme Tecniche per le Costruzioni (in Italian), Ministry of Infrastructures and transportation, Italy 2005.

[5] ISO/TS 16732, Fire Safety Engineering - Guidance on fire risk assessment, 2005.

[6] SFPE- Society of Fire Protection Engineers, Handbook of Fire Protection Engineering, National Fire Protection Association, 3rd Edition, 2002.

[7] ISO/PDTS 16733, Fire Safety Engineering - Selection of design fire scenarios and design fires, Committee draft 2005.

[8] Sundström, B., A methodology to create a design fire, NIST Workshop on Fire Growth and Spread on Objects, March 4-6, 2002.

[9] SFPE- Society of Fire Protection Engineers, Engineering Guide to Application of Risk Assessment in Fire Protection Design, *Review Draft*, October 2005.

[10] ASTM- American Society for Testing Materials, E1776 Standard Guide for Development of Fire-Risk-Assessment Standards, 2007.

[11] NFPA- National Fire Protection Association 551, Guide for the Evaluation of Fire Risk Assessments, Edition 2007.

[12] Gkoumas, K., Crosti, C. and Bontempi, F., Risk Analysis and Modelling Techniques for Structural Fire Safety, in Proceedings of the CST2008 & ECT2008 Conferences, Athens, 2-5 September 2008.

GENERALISED THERMAL AND STRUCTURAL FIRE ANALYSIS WITH GENISTELA AND GENISTRUC

Hong Liang, Stephen Welch, Löic Faure, Martin Gillie

University of Edinburgh, BRE Centre for Fire Safety Engineering, Edinburgh, UK

INTRODUCTION

Increasing interest in assessing the performance of structures in fire is driving the development of an array of modelling methodologies to be used in fire safety engineering design. Whilst traditionally most code-based design has been invoked simple calculations, referencing measured fire performance in standard tests, the progressive shift towards performance-based design has opened the door to use of advanced methods exploiting numerical models. These approaches will not replace standard testing, but they can already be used in a complementary fashion, to extend the application of test data, or in cases where standard test results are not applicable.

Some simplified modelling methods have also been established, such as the protected member equation in Eurocode 3 (EC3) [1], but as with all semi-empirical methods the results will tend to be conservative and there are of necessity a number of simplifying assumptions. CFD-based methodologies can in principle provide a much more detailed description of the thermal environment in fire and the effects of localised heating, which could be used in conjunction with thermal analysis models to examine structural fire performance. In previous work [2], a dedicated fine-mesh thermal modelling tool, known as STELA (Solid ThErmaL Analysis), has been implemented within the RANS CFD code SOFIE [3]. However, the practical application of these techniques suggests that detailed thermal analysis of structural members in the context of simulations of full-scale building fires remains problematic. This is partly due to the difference of scale between the mesh which can be afforded for the fire and that required for the thermal analysis of the structure, a particular problem with structured meshes, and also the generally high computational demands for coupled analyses. Moreover, existing approaches are limited to consideration of a specific structural arrangement of interest, since it is necessary to define all model parameters in advance. Simulations must be repeated from the beginning if details such as the structural geometry or the thermal properties are changed, a very inefficient procedure.

To overcome the above limitations, a more general and flexible methodology has been developed, still within the context of a CFD fire simulation. This novel methodology is called GeniSTELA (Generalised Solid ThErmaL Analysis) and is currently implemented in SOFIE. It has been verified and validated as reported elsewhere [4-6]. Moreover, the computational requirements are also assessed considering a number of aspects, such as the number of simultaneous parametric cases, the required frequency of the GeniSTELA steel temperature field computation and, hence, the overall balance between fluid and solid-phase analysis.

This paper includes a demonstration of the intended operation of GeniSTELA in application to a hypothetical scenario, with simultaneous computation of 72 parametric variants. GeniSTELA provides a large amount of output, including the predicted steel temperature field throughout the compartment for all combinations of structural members and protections considered. By this means, an efficient approach to determining the worst case steel temperatures is provided, with no requirement to repeat simulations of the fire itself. On the

other hand, a special methodology is required to directly use of those outputs for mechanical analysis of structures. An extended methodology called GeniSTRUC (Generalised STRUCture analysis) is developed, exploiting the closed form solutions for simple structural forms (a connected beam/column assembly). It is currently used to predict the plastic collapse and buckling behaviour. For validation, the method has been compared with the FEM method (ABAQUS). A comparison to the experimental measurements obtained in the CTICM external column fire tests is also undergoing.

1 GENISTELA

As mentioned elsewhere [4-6], the GeniSTELA methodology is based on computation of a set of "steel temperature field" parameters within the whole of the calculation domain, accommodating, by means of simultaneous calculations, both uncertainties in the input parameters and possible variants to the specification. Hence the need for repeat simulations is bypassed. Furthermore, by predicting the member temperatures at each point in space the limitations of existing methods with regards to the position of the structural component are overcome. Considering the potentially great computational costs associated with the large numbers of thermal analysis calculations required (equal to the number of gas-phase cells times the number of variants studied in the simultaneous calculations), approximate methods are employed to reduce the full 3D thermal response problem down to treatments which are essentially 1D but which include appropriate representations of the heat transfer processes in the other dimensions to reconstruct a quasi-3D solution. The computations are performed in each gas-phase CFD cell in the computational domain. The heat transfer within the structure and CFD calculation are solved separately and then coupled together by exchanging data, such as temperatures and velocities at their mutual boundaries at the end of the time step. For generalisation and accuracy, heat transfer submodels are also implemented within GeniSTELA to treat the important factors which might have great impact on the transient thermal response, such as the convection coefficient and material thermal properties. The details of the model development are described previously [4-6]. Figures below provide schematics which reference the various concepts of quasi-3D model (Fig. 1 for 1D model and 2 for 2/3D corrections).

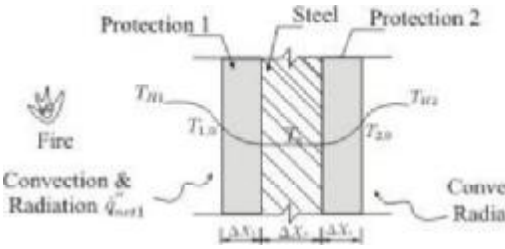

Fig. 1. Schematic of heat transfer for 1D model

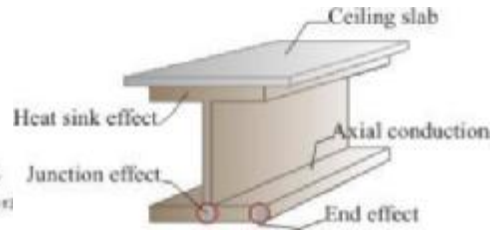

Fig. 2. Correction effects for 2/3D

2 APPLICATION TO HYPOTHETICAL SCENARIO

2.1 Background

GeniSTELA has been applied to a 'hypothetical benchmark scenario' defined in the RFCS FIRESTRUC project [7]. This involves a series of steel tubes and I-profile columns and beams inside an open-ended compartment 30 m by 20 m in floor area and 10 m high. The fire was specified as a heptane pool in a 5-m square tray, following a t-squared fast-growing curve

and reaching 30 MW in 800s, remaining steady thereafter. A more detailed description of the test scenarios is available in the report [7]. In this work, as a demonstration of GeniSTELA for practical use, the methodology was applied in the reported case with fire at location A, representing the non-symmetrical fire position.

72 simultaneous parametric variants were examined, spanning different steel sections and protection properties, etc, with a single parameter modified from the defaults in each case. For the default case, a IPE B 500 section long beam was adopted with Fendolite MII fire protection material with 1-hour fire rating thickness. Eurocode properties were assumed for the steel and the surface emissivity was set as 0.8. The other parameters varied where the steel section (dimensions and weight), protection materials specification including material type (sprayed fibre, board and intumescent) and thickness, together with the thermal-related properties of the material, including moisture content, thermal conductivity, specific heat, density and surface emissivity. On case without protection was also analysed, using a simpler variant of the standard GeniSTELA analysis, to provide a limit for the expected worst case condition and allowing the comparison with the 'hypothetical benchmark test' results obtained from other models in earlier work [7].

Various locations on the surfaces of beams and columns studied in the earlier work were examined for comparison of steel temperature field predictions, as shown in Fig. 3 below:

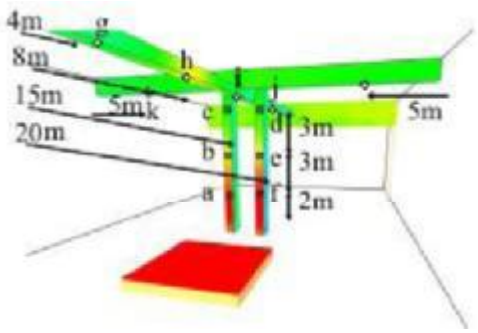

Fig. 3. Locations studied

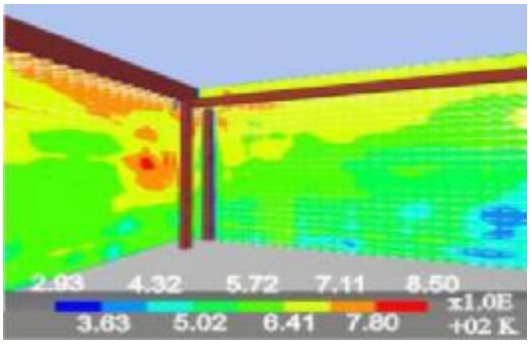

Fig. 4. Example graphical output from GENISTELA at 3600 s

2.2 Results and analysis

The simulation provided steel temperature field results for all parametric cases within an affordable computational time (roughly double that required for the fire itself, when the steel temperature was computed at the end of each timestep). Fig. 4 is an illustration of the results, which shows the calculated steel temperature field and flowfield vector distributions at 3600s, for the default case. As expected, increased temperatures are predicted at locations close to the fire source and in the hot layer, confirming that these are the most critical areas for structural member performance for this particular fire scenario.

The results presented below (Figs. 5-8) focus on the steel temperatures at some of the locations specified in Fig. 3. The results have also been compared with EC3 [1] method and those obtained from other modelling methodologies exploited in the FIRESTRUC project [7], whilst model sensitivities have been examined and demonstrated.

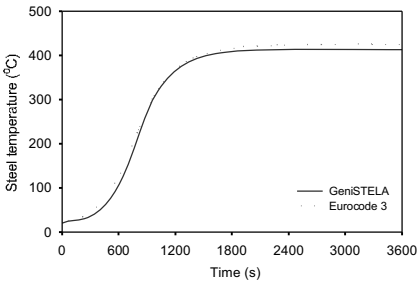

Fig. 5. Comparison of steel temperatures for unprotected member between GeniSTELA and EC3 at location g

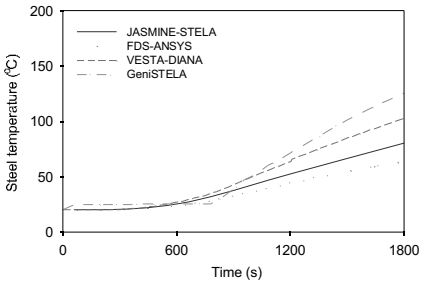

Fig. 6. Comparison of steel temperatures for unprotected member between GeniSTELA and other models at location e

Fig. 5 shows that the prediction for unprotected steel is in good agreement with the EC3 method the unprotected steel. These temperatures exhibit the same trend as those obtained using other code pairs, see Fig. 6.

Regarding structural fire design, the protected cases are more of interest. A series of predicted steel temperatures at various locations for the default case have been studied, including locations a, c, g, h and j (see Fig. 3). These cover most typical steel structure locations of interest during a fire, i.e. either structure in a cold layer or hot layer, above the fire source or away from the fire source, close to the ventilation opening or far away from the opening. The results also suggest that higher temperatures would be expected at the locations close to the fire source in the hot layer.

Sensitivity study has been carried out. Fig. 7 and 8 demonstrates some of the key factors that affect the prediction results, based on location g. The sensitivity study results indicate the final steel temperature is strongly affected by the structural element geometry and the fire protection materials as well as the thermal conductivity. The moisture content could be an important factor within a certain temperature range before the moisture has vanished. Emissivities in the range 0.1 to 1.0 were examined and differences of up to 20% found in the later stages of the heating. Effects are much smaller initially, when convective heat transfer is dominant, consistent with the findings by Staggs and Phylaktou [8]. The results guide the definitions of default parameters for reasonable worst cases and suggest the possible exploitation opportunities in structural fire design.

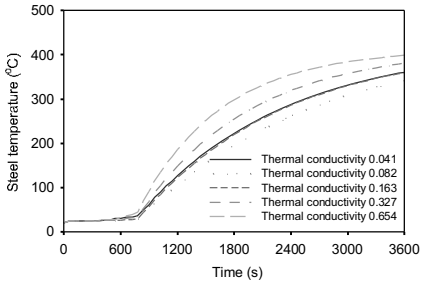

Fig. 7. Effect of protection thermal conductivity on calculated steel temperatures

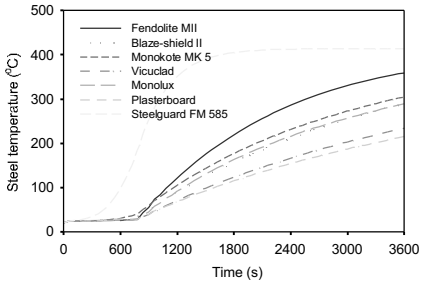

Fig. 8. Effect of protection type on calculated steel temperatures at 1 hour fire rating thickness

3 GENISTRUC

3.1 Methodology

The ultimate goal of this work is to assess the mechanical performance of structures in fires, but so far no failure criteria beyond traditional critical temperature methods have been considered. In light of the advantages of GeniSTELA, the potential for using simplified structural analysis methods, exploiting closed-form solutions, to establish a more robust means of predicting the ultimate structural performance within this generalised framework is explored and a generalised methodology called GeniSTRUC is proposed.

GeniSTRUC is developed as a 'simple' method by considering a simplified structural assembly as a whole, cf. the method of Quiel and Garlock [9]. A simplified model is adopted for representing interactions between the two components, adding a spring where appropriate to represent the flexural stiffness and strength of the column. The members are thereafter subjected to thermal expansion and thermal bowing actions due to the temperature elevation. Each part of the component is then analysed separately, with the stiffness of the spring varying according to time and temperature in order to represent the interaction. Under the temperature elevation, the beam expands and as a result of the partial restraint brought by the column, an axial force is developed in the beam. The beam is considered to be composed of different segments which are in fact corresponding to the meshing of GeniSTELA. As the temperature elevation is different in each segment, the Young's modulus and the ultimate strength are different. Then the ultimate plastic moment (Mu) can be computed for each segment and is a function of the geometry of the cross section, the axial force and the ultimate strength of the beam. The optimum number of segments is chosen by the user depending on the affordable computing time and the required accuracy. The method could also be applied to the column, where the lateral force is brought by the expansion of the beam instead.

3.2 Analysis

The model has been implemented in a spreadsheet and compared with FEA (Finite Element Analysis) modelling using ABAQUS. Its performance has also been examined in a validation scenario based on the CTICM external column fire tests though the work is still undergoing.

Table 1 shows the comparison between GeniSTRUC and ABAQUS regarding to the failure time. The prediction difference is within reasonable range and generally conservative for GeniSTELA.

Table 1. Failure time prediction comparison

Load (KN)	Time of failure (s)	
	GeniSTRUC	ABAQUS
175	570	600
180	510	600
185	420	480

4 CONCLUSION

Along with the case study, the simulation results demonstrate the simultaneous computation capability of GeniSTELA. The detailed method-to-method comparison results demonstrate

the practical use of GeniSTELA in terms of the prediction sensitivities and the associated computational costs, hence the possible use in the field of the structural fire design.

In addition, the framework of GeniSTRUC has been formed to assess the structural integrity by doing plastic and buckling analysis, using temperature field results from GeniSTELA, while taking into account its direct surroundings. GeniSTRUC has been proved to be a very efficient tool for structural analysis as the extension of GeniSTELA, based on the initial tests.

Overall, GeniSTELA and GeniSTRUC are demonstrated as comprehensive but practical tools for structural fire design, providing far more flexibility in assessing the thermal and mechanical responses of steel structures to fire than has been available hitherto, with potential to improve the efficiency and safety of the relevant constructions.

REFERENCES

[1] BSI. Eurocode 3: Design of steel structures – Part 1-2: General rules – Structure fire design. British Standards Institution. 2005.

[2] Kumar S, Welch S, Miles SD, Cajot L-G, Haller M, Ojanguren M et al. Natural Fire Safety Concept - The development and validation of a CFD-based engineering methodology for evaluating thermal action on steel and composite structures, report No. ISBN 92-894-9594-4. European Commission, 2005. 150 pp.

[3] Rubini PA. SOFIE-simulation of fires in enclosures. Cranfield University. 1997.

[4] Liang H. GeniSTELA - A generalised engineering tool for thermal analysis of structural members in fire. PhD thesis, University of Edinburgh, 2008. 215 pp.

[5] Liang H, Welch S. A novel engineering tool for thermal analysis of structural members in natural fires. *Proc 4th Int Workshop on Structures in fire*. Aveiro, Portugal, 2006.

[6] Liang H, Welch S, Stratford T, Kinsella EV. Development and validation of a generalised engineering methodology for thermal analysis of structural members in fire. *Proc 5th Int Seminar Fire and Explosion Hazards*. Edinburgh, UK, 2007.

[7] Welch S, Miles SD, Kumar S, Lemaire T, Chan A. FIRESTRUC - Integrating advanced three-dimensional modelling methodologies for predicting thermo-mechanical behaviour of steel and composite structures subjected to natural fires. *IAFSS 9*, Karlsruhe, Germany, 2008.

[8] Staggs JEJ, Phylaktou HN. The effects of emissivity on the performance of steel in furnace tests. *Fire Safety J. vol. 43, pp. 1-10,* 2008.

[9] Quiel SE, Garlock MEM. A performance-based design approach for steel perimeter columns subject to fire. *Proc 4th Int Workshop on Structures in fire*. Aveiro, Portugal, 2006.

Application of Structural Fire Engineering, 19-20 February 2009, Prague, Czech Republic

Experimentation of the Subway Smoke Control System

Ni Zhaopeng，Kan Qiang

Tianjin Fire Research Institute, the Ministry of Public Security, Tianjin, P.R.China

INTRODUCTION

As a fast, comfortable urban transport tool with big capacity, subway has a history of more than a hundred years. It has been widely adopted in most of the major developed countries or regions and has been playing an important role in easing urban traffic pressure. However, because of the special structure of the subway, in the event of fire, large amount of smoke is generated, heat is not easy to spread, firefighting and rescue work is difficult to be carried out; serious casualties could be caused. In a subway fire, smoke is the major factor threatening life safety. It not only impedes people's sight for escape, causes suffocation, but also makes the fire-fighting and rescue work difficult[1]. As one of the major fire facilities in subway, Smoke control system plays an irreplaceable role in the guarantee of the safety of people and facilitating the fire-fighting and rescue work. Therefore, field test were done by Tianjin Fire Research Institute of the Ministry of Public Security to analyze the performance of the smoke control system in a new subway before it was put into operation. The field test and numerical simulation analysis could not only provide an objective and accurate evaluation, but also help us to find problems and to put forward suggestions for improvement. The research will also provide basic data for amendments to the related existing technical specifications of China.

1 FIELD TEST PROCEDURE

1.1 Brief introduction to the subway station

The subway station is two-story island-type. The concourse is on the first floor of the underground. It has 4 entrance/exits to the ground, namely 1,2,3 and 4. The second floor of the underground is the platform. Two stairs and two escalators connect the platform and the concourse, namely stair 1 and 2 and escalator 1 and 2. The layout of the concourse and the platform is shown in Figure 1and Figure 2 respectively.

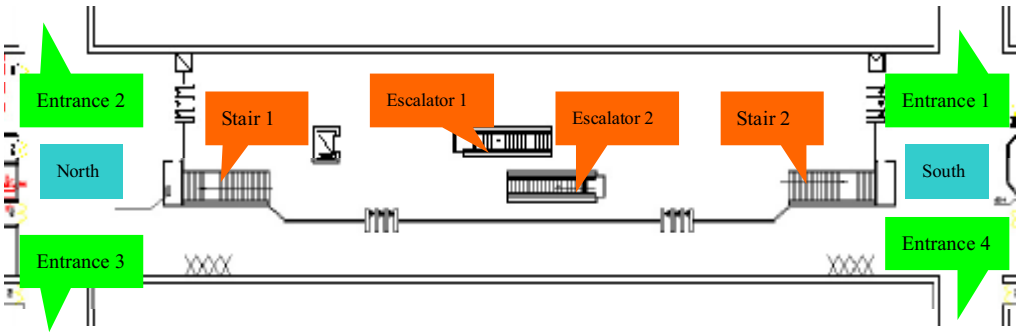

Fig.1. Layout of the concourse

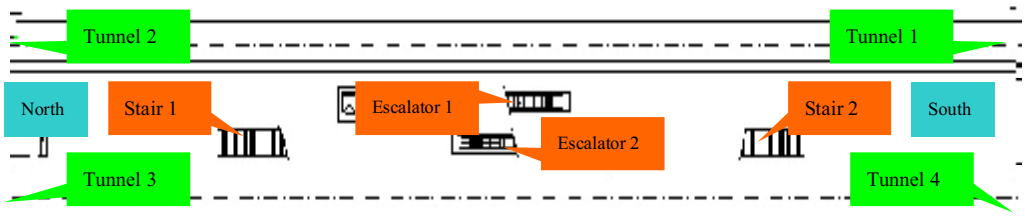

Fig.2. Layout of the platform

According to the design, the platform and the concourse were respectively divided into 2 separate smoke-proof divisions -A, B and C, D, with an area of 537m^2, 560m^2, 854m^2 and 856m^2 respectively. The concourse has exclusive exhaust ducts, arranged in two rows with a total of 52 outlets; the ventilator at the top of the platform, with 66 outlets in two rows, serves as a smoke exhauster for the public area. The exhaust ducts at the top of the two tracks, a total of 108 outlets with 54 outlets for each exhaust duct, also used to exhaust smoke. The main smoke-proof parameters of the station are shown in Table 1:

Table 1 Main parameters of smoke proof/exhaust design of the subway station

Location	Area of smoke-proof division（m^2）		Arrangement of exhausters, exhaust ducts and outlet	
Platform floor	smoke-proof division A	smoke-proof division B	Over platform	Over tracks
	537m^2	560m^2	2 rows of exhaust ducts 33×2 outlets	2 rows of exhaust ducts 54×2 outlets
Concourse floor	smoke-proof division C	smoke-proof division D	2 rows of exhaust ducts 26×2 outlets	
	854m^2	856m^2		

2.2 Test method

On-site tests can check the installation and operation of the smoke prevention/exhaust system of the subway, as well as the difference between the design and actual effects. In order to simulate the real circumstances of the fire, the test were carried out in 2 ways: one is to use smoke cake to produce smoke with industry alcohol auxiliary heating method to increase buoyancy of the smoke. The other is to use wood crib to simulate the actual fire with a certain scale.

Baggage fire commonly occurred in the concourse and platform of subway station. The average fire scale of the common luggage fire was determined as 200kW~400kW according to some related research report[2]. In order to obtain a better repeatability, wood crib fire was applied to simulate the actual fire of this scale.

Wood crib was prepared in accordance with national standard *Characteristics and tests for transportable fire extinguishers*(GB 8109-1987)[3]. Through the results of several different sizes of wood crib fire tests with large-scale calorimeter, the size of the wood crib used in the actual test was defined as: 500mm × 1300mm × 6-layers, the scale of the fire were 0.5MW ~ 0.7MW.

As the smoke produced by wood crib was relatively different from that produced in the actual fire, it wasn't able to get a good result in testing the performance of the station's smoke proof/exhaust system. Therefore, wood crib fire plus smoke cake methods was used in hot smoke test.

2.3 Contents of the full-scale test

According to the purpose of the test as well as the structure of the station, 3 scenarios (smoke-free,

cold smoke and hot smoke) were adopted at 2 areas- concourse andplatform.

1）Performance test of ventilation status of the concourse and platform at normal condition: To test the performance of exhaust system and internal environmental status of subway station under normal condition;

2) Smoke-proof division test: in case of fire in platform/concourse, hot and cold smoke tests were carried out at typical locations such as the stair exit, escalator mouth, platform and concourse center so as to test the actual effects of the smoke-proof divisions and smoke-proof Facilities;

3) Cross-section wind speed measurement on the concourse and platform: in case of fire in platform/ concourse, hot and cold smoke tests were carried out at typical locations such as the stair exit, escalator mouth, platform and concourse center so as to observe the flow of gas and to measure continuously the cross-section wind speed of the stairs and the escalators;

3 Full-scale test of the station

3.1 Concourse fire

3.1.1 ventilation / smoke exhaust system operation mode of the station

In case of concourse fire, the station concourse's ventilation / smoke exhaust system adopts the smoke exhaust mode, to stop air supply and exhaust the smoke of the concourse through the smoke tower to the ground. At the same time, the ventilation/smoke exhaust system adopts the wind blowing mode, so that smoke will not spread to the platform. the fresh air enter the concourse through the entrances/exits of the platform in order to facilitate the evacuation of passengers from the concourse to the ground. The smoke control method of the concourse is as shown in Table 2:

Table 2 smoke control mode in concourse fire

Location of fire source	Exhausters in concourse		Exhausters in platform		Exhausters above tracks	
	Scenario	Outlet number	Scenario	Outlet number	Scenario	Outlet number
concourse	Smoke exhaust	52	Wind supple-ment	34 at south end	—	—

3.1.2 Test results

In case of concourse fire, the main content of the test is the wind speed of the smoke outlet in the concourse. During the test, the wind speed of 5 different locations for each smoke outlet among 52 outlets was measured. After filtering and data processing, the average wind speed of the smoke outlets in concourse was 3.7m/s.

The dimension of smoke outlets in the concourse was 500mm × 500mm with deflection grilles. Its designed wind capacity was 5262m^3/h. the average wind speed measured in the test was 3.7m/s, which was equivalent to the wind capacity of 3330m^3/h (55.5 m^3/min)-about 63% of the value of the design value. According to the actual construction area of the concourse (1710m^2), the actual amount of smoke exhaust is calculated as (55.5m^3/min × 52) / 1710 m^2 = 1.69 m^3/m^2 min.

Test results showed that the smoke ventilation/smoke exhaust system designed for the concourse couldn't meet the design requirements. The duct's pressure loss and the fan performance were tested. Only to find that when the concourse's ventilation/smoke exhaust system was switched to the fire mode, serious leakage occurred at valves and ducts, and the exhaust amount couldn't meet the design requirements.

After the adjustment and improvement of the system, another test was carried out. The average wind speed of the concourse's smoke outlet increased to 4.04m/s; the air flow of a single smoke outlet is 3636m^3/h (60.6 m^3/min), which was about 70% of the value of the design. As a result, the smoke exhaust capacity of the concourse measured in the test was (60.6m^3/min × 52) / 1710 m^2 = 1.84 m^3/m^2 min, which still couldn't meet the design requirements.

3.1.3 Hot smoke test in case of concourse fire

In case of concourse fire, the hot smoke test was carried out. Figure 3 showed the smoke movement in the concourse during the hot smoke test.

According to the observation, the visibility in the concourse was less than 2m when the fire developed to its medium-term, which meant that the ventilation/smoke exhaust system behaved badly in fire. By improving the ventilation/smoke exhaust system, the smoke exhaust capacity was improved obviously, and the visibility reached to 5m. However, smoke at entrance/exit 1 gathered and settled due to the incompletion of the entrance/exit, which led to poor air circulation.

Figure.3. smoke movement in concourse during hot smoke test
(fire source at the center of the concourse)

3.2 Platform fire

3.2.1 ventilation / smoke exhaust system operation mode of the station

In case of platform fire, the ventilation / smoke exhaust system of the platform and the hot smoke exhauster at top of the tracks adopted smoke exhaust mode. The smoke in the platform was exhausted through the smoke tower to the ground. Fresh air entered the platform through the entrances/exits, concourse, and mouths between the concourse and platform. The smoke control method of the platform is shown in Table 3:

Table 3 Smoke control in platform fire

Location of fire source	Exhausters at concourse		Exhausters at platform		Exhausters above tracks	
	Scenario	Outlet number	Scenario	Outlet number	Scenario	Outlet number
platform	—	—	Smoke exhaust	66	Smoke exhaust	108

3.2.2 Test results

In case of platform fires, the wind speed of the smoke exhaust outlets at the top of the platform and tracks was measured. The average wind speed of the smoke exhaust outlets above platform was 3.8m/s, the average wind speed of the smoke exhaust outlets above tracks was 1.65m/s.

500mm × 500mm double layer smoke exhaust outlets, with an designed air capacity of 5454.5m^3/h, were used at the top of the platform. The average wind speed measured in the test was 3.8m/s, which was equivalent to the wind capacity of 3556.8m^3/h (59.3 m^3/min)-about 65% of the value of the design. According to the actual construction area of the platform (1097m^2), the actual amount of smoke exhaust of the smoke exhauster at the top of the platform was calculated as (59.3m^3/min× 66)/1097 m^2=3.56 m^3/m^2·min.

500mm × 1000mm smoke exhaust outlets were used at the top of the tracks. The average wind speed measured in the test was 1.65m/s, which was equivalent to the wind capacity of 2970m^3/h （49.5 m^3/min）. The actual amount of smoke exhaust of the smoke exhauster at the top of the tracks was calculated as (49.5m^3/min×108)/1097m^2=4.87 m^3/m^2·min.

In case of platform fire, downward wind speed was tested at different locations of the two stairs and two escalators. According to test results, the actual downward wind speed of stairs was between 0.82 m/s ~ 1.15 m/s.

3.2.3 Cold and hot smoke test in case of platform fire

In case of platform fire, cold smoke test was carried out at the centre of the platform, platform stairs, and the tunnel near the platform respectively. Figure 4 shows the smoke movement observed at the escalator when cold smoke released at the centre of the platform. Figure 5 shows the smoke movement observed at the stairs when cold smoke released at the stairs.

Fig.4. status at the mouth of the escalator under platform cold smoke test（cold smoke source was in the center of platform）

Fig.5. status at the mouth of the escalator under platform cold smoke test （cold smoke source was in the mouth of escalator）

According to the observation, regardless of locations of the smoke source, under the effect of the downward airflow at the stair and escalator mouths and the around retaining walls, smoke was not found spreading to the concourse from the stair and escalator mouths.

In case of platform fire, hot smoke test was carried out with the smoke source at the centre of the platform. Under the joint action of the downward airflow (0.82m/s ~ 1.15m/s) and the retaining wall at the mouths of the stairs and the escalators, no smoke spread from the platform to the concourse when hot smoke released at the maximum heat release rate of 0.5 ~ 0.7MW.

Through the cold and hot smoke tests, we can see that although the measured downward air flow speed at the stair mouths can not meet 1.5m/s, which is stipulated in the national standard "Code for Design of Metro" (GB50157-2003)[4], the existing design achieves the desired results. The evacuation of passengers has been secured and the objectives of stopping the spread of smoke to the concourse through the mouths of the stairs and the escalators have been achieved.

Figure 6 and Figure 7 shows the smoke flow of the platform under the hot smoke test condition. We can see from them that the effect of the smoke-proof divisions divided by the retaining walls is not satisfactory. The entire platform has become one division. The reason for this phenomenon is that the retaining walls were not built above the tracks at the side of the platform, but only built along the centre of the platform.

Fig.6. hot smoke test: south end of platform （the hot smoke source was at the center of the platform）

Fig.7. hot smoke test: north end of platform （the hot smoke source was at the center of the platform）

4 CONCLUSION

Through the systematic full-scale fire test, the newly built subway is able to meet basic requirement for safe evacuation of people in case of a fire. But there are still some problems that need to be further improved. For example, the closeness of the switching valve and ducts of the ventilation / exhaust system should be further dealt with, and the capacity of the smoke exhaust system should be improved; entrance 1 of the station should be constructed timely and be improved to ensure smooth flow of the air and avoid settlement and gathering of smoke; the smoke exhaust effect of the concourse and the smoke-proof division of the platform need to be improved, is necessary to build smoke retaining wall above the tracks near platform. In addition, it has been found from the test that in the existing “code for Design of Metro", the value given for the smoke exhaust volume of platform is low while the downward wind speed at stair mouth is high. We suggest that those requirements should be adjusted.

REFERENCES

[1] Tianjin Fire Research Institute, Case Study on Typical Subway/Tunnel Fire, *Research Report of Research project of the Ministry of Public Security*, 2003.

[2] Tianjin Fire Research Institute, Experimental Study on Baggage Fires of Subway Passenger, *Research Report of 10th five-year plan of China*, 2006.

[3] Ministry of Public Security of the P.R.China, GB 8109-1987: Characteristics and tests for transportable fire extinguishers, 1987.

[4] Ministry of Construction of the P.R.China, GB 50157-2003: Code for Design of Metro, 2003.

Experimental Study on Baggage Fires of Subway Passenger

Kan Qiang，Ni Zhaopeng

Tianjin Fire Research Institute, the Ministry of Public Security, Tianjin, P.R.China

INTRODUCTION

Subway fire safety has been paid much attention to because of its special structure. There are many causes that result in subway fire, among which baggage fire in the platform and concourse is one of them. In order to find out the rule of baggage fire, typical baggage fire tests were carried out. Fire heat release rate curves of baggage fire were obtained so as to provide the basis for fire protection design of subway station.

1 BAGGAGE FIRE TEST

1.1 Field survey

To ascertain the categories and the weights of subway passengers' baggage, field survey on Beijing Subway was carried out. The idiographic survey locations were subway stations of Beijing railway station and Xizhimen subway station. Questionnaires, baggage weighting and video recording were used to do the survey. Some survey results are as follows:

Table 1 average weights of passengers' baggage

Subway station	Beijing railway station	Xizhimen subway station
average weight of passengers' baggages /kg	3.9	1.67

Table 2 Categories and average weights of baggage in the subway station of Beijing railway station

Categories of baggage	keister	satchel	plastic bag	briefcase	suitcase
average weight /kg	1.22	3.01	2.5	2.49	6.37

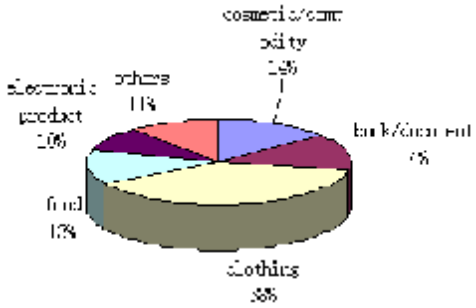

Fig.1. Categories of baggage

1.2 Determination of categories and weight of baggage

Fire tests on shopping mall for clothing and shoes have been carried out in Tianjin Fire Research Institute[1]. One test was 5kg mixed quality clothing burning on the shelf. According to the test, the heat release rate reached the maximum 98.67kW when the clothing was ignited 251s later. The result proved that both 3.9kg -- average weight of the survey result of subway station of Beijing railway station and 1.67kg --average weight of the survey result of Xizhimen station could only cause small scale fire, which should be put out easily. The worst case would be fires caused by large baggage. Therefore, two kinds of baggage were considered. As shown in Table 3, 6.37kg was the average weight of suitcase; 11.00kg was the largest baggage in the survey.

Table 3 Categories and weights of baggage of the tests

weight of a baggage (kg)	clothing (kg)	food (kg)	Electronic product (kg)	book/document (kg)	Cosmetic/commodity (kg)	other (kg)
6.37	2.42	0.83	0.64	0.89	0.89	0.70
11.00	4.18	1.43	1.10	1.54	1.54	1.21

Different types of goods in baggage were identified as follows: 'clothing' were clothes made with different materials, mainly cotton clothing; 'food' was instant noodles and biscuits; 'electronic product' were demolition materials of obsolete computers; 'book and document' were books, newspapers, etc.; 'cosmetics and commodity' were sanitary towels. As 'other' items can not be precisely defined, so the synthetic bag was regard as other goods. If the weight of synthetic bag was less than the required weight, then clothing were added.

clothing（dress/bedsheet/cap）

cosmetic/commodity(sanitary napkin)

food(instant noodles)

book/document(book/newspaper)

electronic products (demolition materials of obsolete computers)

one baggage

Fig.2. Goods in Test

1.3 Test method

The ignition sources of the tests were cotton balls dipped with petrol. In the process of fire tests, the whole process of fire development was recorded. In some tests, fire sources were taken photos by infrared camera. Fire heat release rates were measured by large-scale calorimeter, temperatures around the fire source were measured by K-sheathed nickel chromium - nickel silicon thermocouples.

Fig.3. Large-scale calorimeter

Fig.4. Data acquisition instrument

A total of 6 group of tests were carried out. Scenarios were shown in Table 4. Forms of baggage's location of the tests were shown in Figure 5~Figure 7.

Table 4 Test scenarios

NO.	1A	2A	3A	1B	2B	3B
Test equipment	Large-scale calorimeter					
Pieces of baggage	one piece of baggage（6.37kg）	Two pieces of baggage (6.37kg for every baggage)	three pieces of baggage(6.37kg for every baggage)	one piece of baggage（11.00kg）	two pieces of baggage(11kg for every baggage)	three pieces of baggage(11kg for every baggage)
goods in baggage	categories and weights of goods in every baggage were determined according to Table 3					
placement	stack on shelves					
ignition sources	cotton balls dipped with petrol					
place of ignition sources	clothing in the baggage	clothing in any of the baggage	clothing in the middle baggage	clothing in the baggage	clothing in any of the baggage	clothing in the middle baggage

Fig.5. Test 1A/1B

Fig.6. Test 2A/2B

Fig.7. Test 3A/3B

2 TEST RESULT ANALYSIS

2.1 Test result of series A

A total of 3 groups of tests were carried out in series A tests. The main measurement data were shown in Table 5.

Table 5 Test result of series A

Test NO.	Maximum heat release rate（kW）	Time of the heat release rate reached the maximum(s)	Maximum temperature (℃)	Time of the temperature reached the maximum(s)
1A	—	—	60	228
2A	196	392	81	454
3A	324	408	152	342
Note: Because the weight of baggage in Test 1A was light, the heat release rate was less than the measuring range of large-scale calorimeter, exact measurement result was not gained.				

Figure 8 showed the heat release rate curves of Test 2A and Test 3A. It showed that the maximum heat release rate of Test 3A was 1.65 times of that of Test 2A. The fire growth rate of Test 3A was more or less the same as the slow speed t^2 fire, while the fire growth rate of Test 2A was more or less the same as the medium speed t^2 fire at the first 140s, but it decreased after 140s. When the heat release rate of two groups of tests reached their peak values respectively, peak value of Test 2A lasted for a longer time than that of Test 3A. The time of the heat release rate of Test 2A reached its maximum heat release rate was almost the same as that of Test 3A. Test 3A lasted slightly longer than Test 2A.

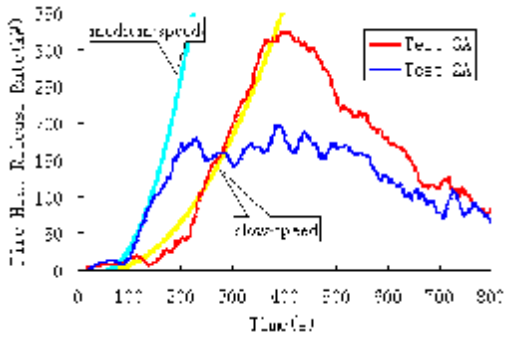

Fig.8. Comparison of heat release rate curve of test series A

2.2 Test result of series B

A total of 3 groups of tests were carried out in series B tests. The main measurement data were shown in Table 6.

Table 6 Test result of series B

Test NO.	Maximum heat release rate（kW）	Time of the heat release rate reached the maximum(s)	Maximum temperature (℃)	Time of the temperature reached the maximum(s)
1B	250	326	157	247
2B	262	381	119	501
3B	356	570	207	690

From Table 6, although the number of baggage of Test 2B was more than that of Test 1B, but the maximum temperature of 2B tests was less than that of Test 1B, which may be caused by the location of the baggage. In Test 1B, a piece of baggage was just under a thermocouple, so the temperature measured by that thermocouple was higher; In Test 2B, two pieces of baggage were put

in the bottom of both sides of a thermocouple, and the location of those two pieces of baggage had a certain angle with other thermocouples, so the temperature measured by that thermocouple was lower.

Figure 9 showed the heat release rate curves of 3 groups of tests of series B. The maximum heat release rate of Test 2B and Test 3B were 1.05 times and 1.42 times of that of Test 1B respectively. The fire growth rate of Test 1B and 2B were between slow and medium speed t^2 fire. The fire growth rate of Test 3B was less than slow speed t^2 fire. However, with the full combustion of the fuel, the fire growth rate of Test 3B was faster than that of Test 1B and Test 2B.

In Test 1B, 2B and 3B, the time of the heat release rate reached their maximum values lagged one after another. When the heat release rate of Test 1B reached the maximum value, it decreased rapidly. While Test 2B and Test 3B fire lasted longer because the number and weight of the baggage was more than that of the Test 1B. The duration of Test 3B was the longest.

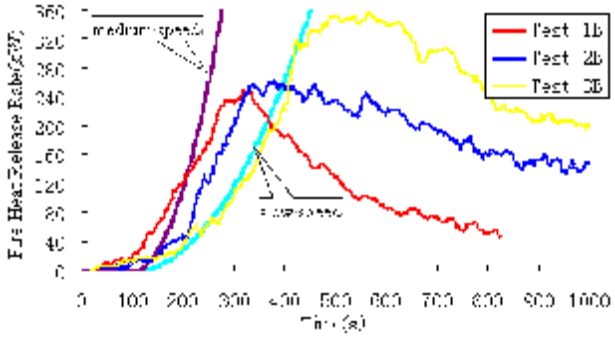

Fig.9. Comparison of heat release rate curve of test series B

2.3 Comparison of test results of Series A and Series B

The test conditions of Test 2A and Test 2B, Test 3A and Test 3B, including the number of baggage, the categories of goods and the location of baggage were the same respectively, only the weight of individual baggage was different. Figure 10 and 11 showed the heat release rate curves of Test 2A and Test 2B, Test 3A and Test 3B respectively. Figure 10 showed that the heat release rate curves of Test 2A and Test 3A were very similar, not only in the growth stage but also in the decay stage. Figure 11 showed that the overall trend of heat release rate curves of Test 3A and Test 3B was similar. Compared Test series A with Test series B, the maximum heat release rate of Test series B was bigger. The maximum heat release rate of Test 2B was 1.34 times of that of Test 2A. While the maximum heat release rate of Test 3B was 1.10 times of that of Test 3A. The time of heat release rate of Test series B to reach its peak value was a litter later than that of Test series A.

Compared Figure 10 with Figure 11, the similarity degree of the heat release rate curves of Test 3A and Test 3B was less than that of Test 2A and Test 2B. Furthermore, the difference between the maximum heat release rate of Test 3A and that of Test 3B was not obvious. This may be caused by the fact that the number and weight of baggage in 3A and 3B was more than that in 2A and 2B and the combustion was inadequate.

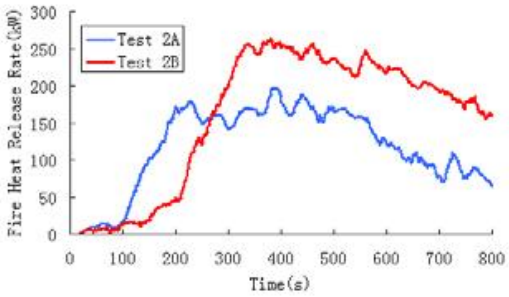

Fig.10. Comparison of heat release rate curves of Test 2A and Test 2B

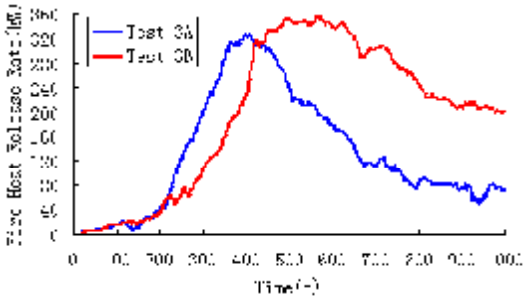

Fig.11. Comparison of heat release rate curves of Test 3A and Test 3B

3 CONCLUSION

The tests proved that ordinary baggage fire scale is 200kW~400kW. Ordinary baggage fire growth rate is between slow and medium speed t^2 fire. In practice, baggage fire growth rate is identified as medium speed fire due to uncertainties.

When using fire simulation software to evaluate building fire safety, heat release rate is an important input parameter. In order to make sure that the evaluate result is reliable and conservative, the chosen heat release rate should consider the worst case. In reality, baggage in the subway station scatters around without piling up. The worst condition is that one baggage ignites 4 pieces of baggage around it at the same time. The test results show that the maximum heat release rate of the single 11Kg baggage was 250kW. The time of one piece of baggage ignites the adjacent baggage was 57s~127s. Based on the fire heat release rate curve of the 11Kg baggage, the assumption is that one piece of baggage ignites 4 pieces of baggage around it at the same time 57S later. Then the heat release rate curve can be obtained, as shown in Figure 12. Based on Figure 12, the maximum heat release rate is 1.2MW. Considering the safety factor, the maximum baggage fire heat release rate used in subway fire safety evaluation can be defined as 1.5MW. Of course, in other building fire safety evaluation, fire design should consider the fire heat release rate curve gained by test, together with the spatial distribution of baggage in buildings.

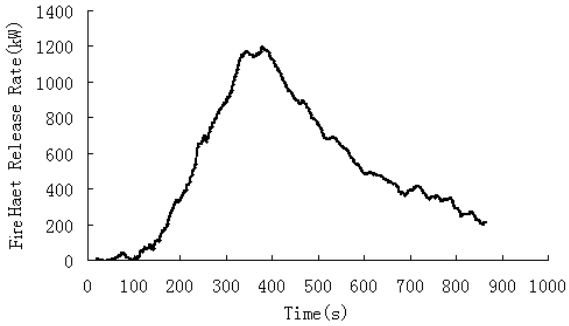

Fig.12. Heat release rate curve of subway baggage fire

REFERENCES

[1] Tianjin Fire Research Institute, Study on Large-scale Underground Shoping Mall Fire , *Research Report of 9th five-year plan of China*, 1999.

Application of Structural Fire Engineering, 19-20 February 2009, Prague, Czech Republic

NUMERICAL SIMULATION ON VERTICAL FIRE SPREAD
Effects of Wall Pier and Overhanging Eave in Preventing Vertical Fire Spread

Huang Xin, Ni Zhaopeng, Lu Shichang

Tianjin Fire Research Institute, the Ministry of Public Security, Tianjin, P.R.China

INTRODUCTION

Building with French windows has the advantages of brightness, wide view and beautiful appearance. Nowadays this kind of structure has been applied in many commercial and residential buildings. However, exterior windows in adjacent stories in this kind of buildings are too close and the fire can spread easily to upper stories.

In order to prevent the fire from spreading vertically through the exterior openings, the minimum height of wall pier is required in the related codes of many countries. NFPA 5000 and *International Building Code* require that openings in exterior walls in adjacent stories shall be separated vertically at least 3 feet (914mm) by spandrel girders, exterior walls or other similar assemblies that have a fire-resistance rating of at least 1 hour[1,2]. Hong Kong's Code also prescribes that there should be a wall pier with height not less than 900mm between the top of one window and the bottom of the next window above. Chinese code requires that an annexed solid non-combustible wall with height not less than 800mm shall be constructed at the outer edge of each floor slab where there is no wall between two windows in vertical directions and a wall pier with height not less than 800mm shall be built up on the upper portion over the opening on the exterior wall of residential buildings[3,4]. However, some kinds of buildings such as buildings with French windows can not satisfy these requirements.

If the wall pier is too short, fire resistant overhanging eave can be built up to replace wall pier for protecting against fire spread on the exterior of the buildings. NFPA 5000 and *International Building Code* require that the overhanging eave should extend horizontally at least 30 inches (762mm) beyond the exterior wall[1,2]. Chinese code requires that the width of overhanging eave should not below 500mm for residential building[4].

Different countries have different requirements for wall pier and fire resistant overhanging eave. In order to study the effects of wall pier and fire resistant overhanging eave in preventing vertical fire spread, computational fluid dynamics (CFD) simulation was performed and typical office fire scenarios, hotel fire scenarios and shop fire scenarios were designed.

1 FDS MODEL SET-UP

1.1 Physical model

CFD simulations were carried out with fire dynamics simulator (FDS), a software package released by the National Institute of Standards and Technology (NIST), USA. It is now a popular CFD tool in fire related researches that describe the flow of smoke and hot gases from a fire. The recent version of FDS 4.0.7 released in March, 2006 was used.

Office fire, hotel fire and shop fire were chosen as simulated objectives. The basic outline of the simulated building is shown in *Fig.1*. The simulated building had six stories. Each storey was 3.4m high and had three rooms. Each room was 6m×6m and had one 3m wide window. The height of the window was changed with the wall pier. The heights of the simulated wall piers (H) were 0.2m, 0.4m, 0.6m, 0.8m, 1.0m and 1.2m, respectively. Both the floor and the side wall were 0.2m thick. There was only a floor between windows in adjacent stories in the simulated building with fire resistant overhanging eave. The widths of the fire resistant overhanging eaves (W) were 0.2m, 0.4m, 0.6m, 0.8m, 1.0m and 1.2m, respectively. The fire source was 4m×4m being set in the middle room of the second

storey. The simulation domain was 18m×9m×21.6m. All grids were 0.2m×0.2m ×0.2m.

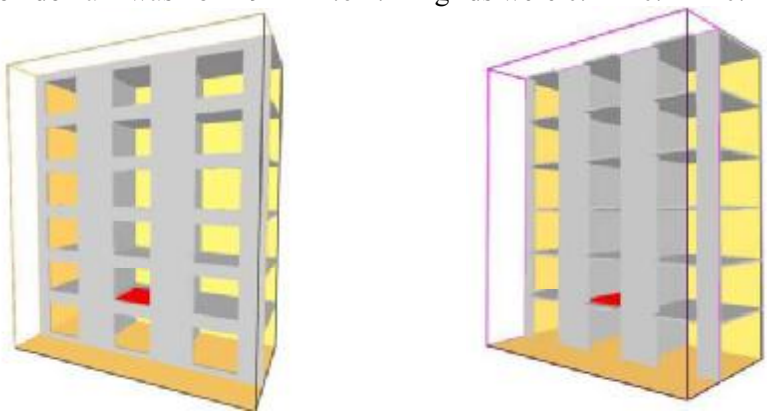

(a) Building without overhanging eave (b) Building with overhanging eave

Fig.1. 3D view of the simulated building (all windows were open)

The simulation adopted the following parameters: ambient temperature (23℃), no wind, concrete side wall and floor, glass window and wood crib fuel. Time for the simulation of all cases (*t*) was 1200s.

1.2 Design fire

The office fire, hotel fire and shop fire were all set as *t*-squared fires (the heat release rate is assumed to be proportional to the square of the elapsed time). The fire growth coefficients of office fire, hotel fire and shop fire were all set as 0.05kW/s^2 by referring to the experiments results of the office fire tests and sofa fire tests performed by NIST[5,6] and the clothes fire tests performed by Tianjin Fire Research Institute[7].

NFPA 92B recommends that the heat release rate per unit area of office fire, hotel fire and shop fire be 290kW/m^2, 249kW/m^2 and 568kW/m^2 respectively[8]. SNZ PAS 4509 recommends that the heat release rate per unit area of office fire and shop fire be 250kW/m^2 and 500kW/m^2 respectively[9]. In our FDS model, the heat release rate per unit area of office fire and hotel fire were both set as 250kW/m^2 and the heat release rate per unit area of shop fire was set as 500kW/m^2. Therefore, the maximum fire sizes of office fire and hotel fire were 9MW and the maximum fire size of shop fire was 18MW.

2 SIMULATION RESULTS

2.1 Effects of wall pier

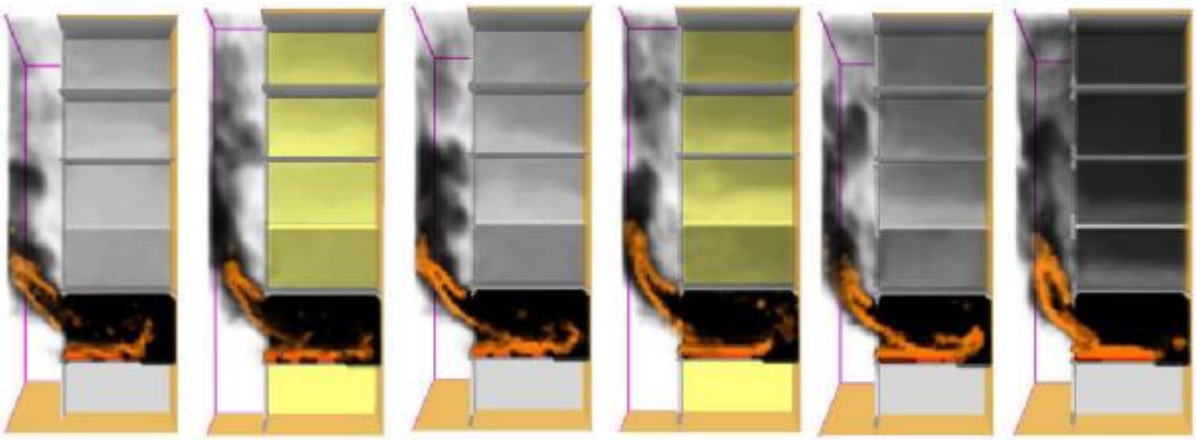

H=0.2m *H*=0.4m *H*=0.6m *H*=0.8m *H*=1.0m *H*=1.2m

Fig.2. Smoke and fire spread profile (all windows were open, 9MW fire, *t*=1200s)

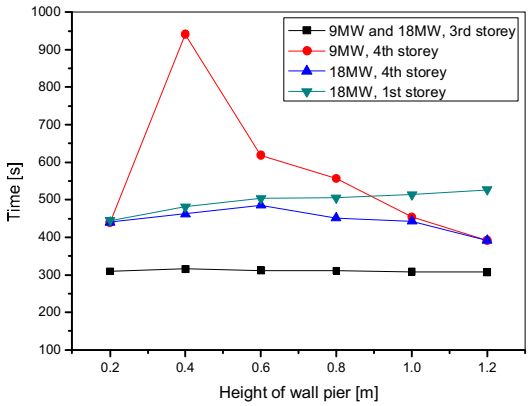

Fig.3. Time to reach 10kW/m^2 at the openings

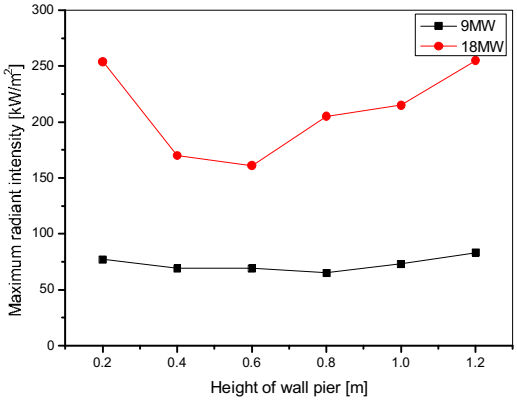

Fig.4. Maximum radiant intensity at the middle opening of the 3rd storey

Fig.2.—*Fig.4.* show the simulation results of the wall piers at different heights with all windows open. After the fire was ignited, the smoke flew out of the fire room with a radial velocity and there was a certain distance between the outside smoke and the exterior wall. The flame also stretched out of the window when the fire was big enough and an angle was formed by the flame and the exterior wall. Since all the windows were open, smoke flew into the rooms at upper stories.

Fig.3. shows the times to reach 10kW/m^2 radiant intensity at the openings at different heights of wall pier. 10kW/m^2 is the minimum radiant intensity to ignite combustibles like thin curtain[10]. The radiant intensity at the openings of the 3rd and the 4th storey could reach 10kW/m^2 in both 9MW and 18MW fire and that of the 1st storey could also reach 10kW/m^2 in 18MW fire. The openings of the non-fire stories were further away from the fire room with increasing the height of wall pier. Therefore, the radiant intensity would decrease with the height of wall pier increased within a certain range. As shown in *Fig.3*, the time at which radiant intensity of the 1st storey reach 10kW/m^2 was prolonged by an increase in the height of wall pier. However, increasing the height of wall pier would induce the outside smoke and the flame closer to the exterior wall at the same time and the radiant intensity at the openings of the upper stories would reach 10kW/m^2 faster. *Fig.2* also shows that the soot density inside the middle rooms of the upper stories would increase with the increases in the height of wall pier because the outside smoke was closer to the exterior wall. As shown in *Fig.4*, the maximum radiant intensity at the middle opening of the 3rd storey first decreased and then increased with the increase in the height of wall pier. The simulation results showed that the optimum heights of wall pier were 0.4m and 0.6m for 9MW and 18MW fire respectively if windows were open. Generally speaking, wall pier could not prevent vertical fire spread effectively with windows open.

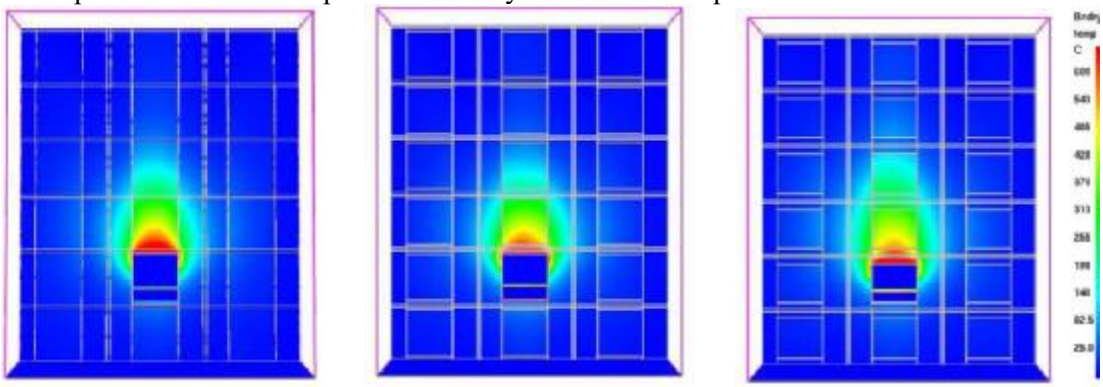

(a) W=0.2m (b) W=0.6m (c) W=1.0m

Fig.5. Temperature profile at the windows (all windows were close, 18MW fire, t=1200s)

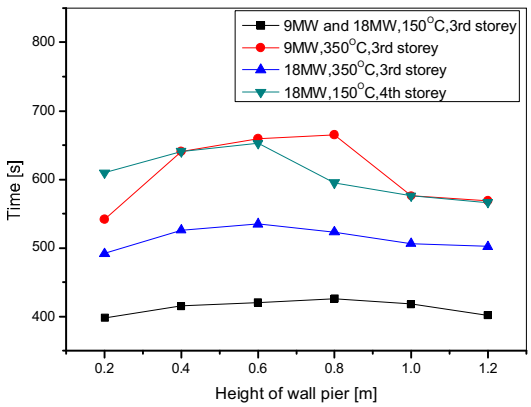

Fig.6 Time to reach 150℃ or 350℃ at the windows

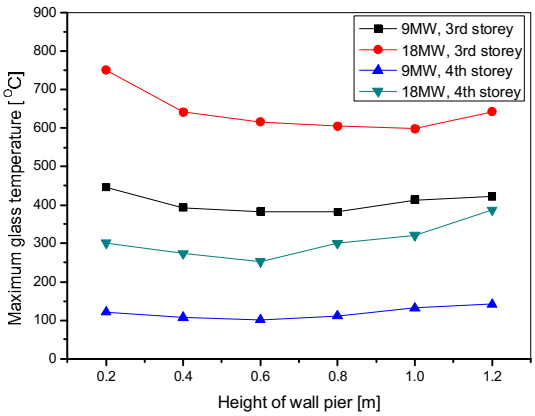

Fig.7. Maximum glass temperature at the middle windows of the 3rd and 4th storey

Fig.5.—*Fig.7.* show that the simulation results of the wall piers at different heights with all windows close. *Fig.5* shows that the temperature on the portion closer to the fire of the windows was higher. With increasing the height of wall pier, the maximum temperatures at the exterior side of the windows first decreased and then increased. The maximum temperature at the middle window of the 3rd storey was lowest when the heights of wall pier were 0.8m and 1.0m for 9MW and 18MW fire respectively. However, for both 9MW and 18MW fire, when the heights of wall pier were 0.6m, the maximum temperature at the middle window of the 4th storey was lowest. And in larger fires, the influence of the wall pier on the maximum temperature was more prominent.

Fig.6. shows the time to reach 150℃ and 350℃ on the exterior side of the middle windows at different heights of wall pier. 150℃ and 350℃ are breaking temperatures for plain glass and tempered glass respectively[11]. The simulation results showed that the radiant intensity has reached 10kW/m^2 when the glass temperature reached the breaking temperature. That is, if the window broke, the fire would be able to spread into the room. In 9MW fire, only the temperature at the middle window of the 3rd storey could reach 150℃. In 18MW fire, only the temperature at the middle window of the 3rd storey could reach 350℃ and that of the 4th storey could reach 150℃. The time at which the temperatures on the exterior side of the windows reached to 150℃ and 350℃ were first increased and then decreased by the increase in the height of wall pier. The simulation results showed that the optimum heights of wall pier were 0.8m and 0.6m for 9MW and 18MW fire respectively if windows were close. Increasing the height of wall pier also could not prevent vertical fire spread effectively with windows close.

2.2 Effects of fire resistant overhanging eave

Fig.8.—*Fig.10.* show that the simulation results of the overhanging eaves at different widths with all windows open. The results showed that fire resistant overhanging eave could prevent vertical fire spread effectively. With the overhanging eave, the fire could not spread to the 4th storey for 9MW fire and to the 1st storey for 18MW fire by radiation. *Fig.9* shows that the time at which radiant intensity of the 3rd and 4th storey reached 10kW/m^2 increased with an increase in the width of overhanging eave. When the width of overhanging eave increased to 0.8m, the fire could not spread to the 4th storey for 18MW fire. *Fig.10* shows that the maximum radiant intensity at the middle opening of the 3rd storey decreased with an increase in the width of overhanging eave, while the decreasing rate was slower if the width was larger. And the effects of the overhanging eave were better for larger fire size. However, too wide overhanging eave would reduce the radial velocity of the smoke when it flew out of the fire room since the overhanging eave would obstruct the upward movement of the smoke. Therefore, increasing the width of overhanging eave would make the smoke flow into the middle rooms of the

upper stories easily and the soot densities and room temperatures in these rooms were higher as shown in *Fig.8*.

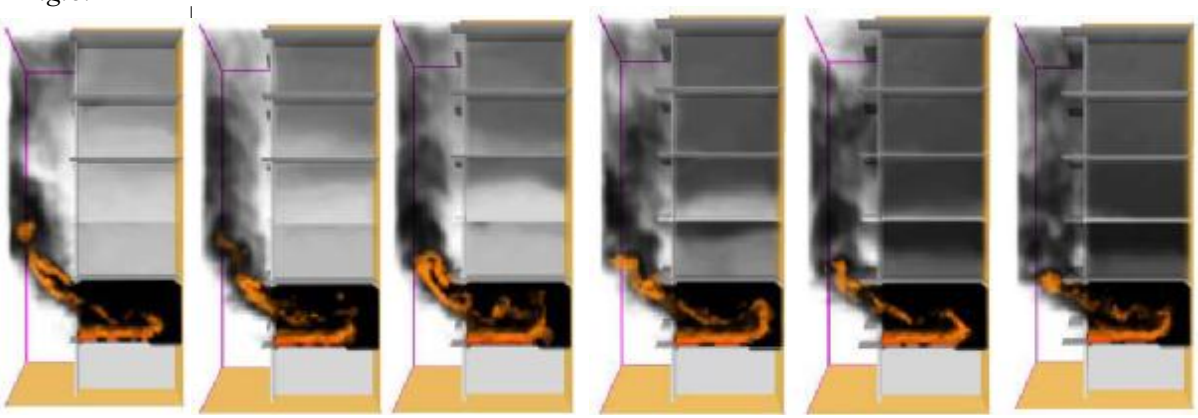

W=0.2m *W*=0.4m *W*=0.6m *W*=0.8m *W*=1.0m *W*=1.2m

Fig.8. Smoke and fire spread profile (all windows were open, 9MW fire, *t*=1200s)

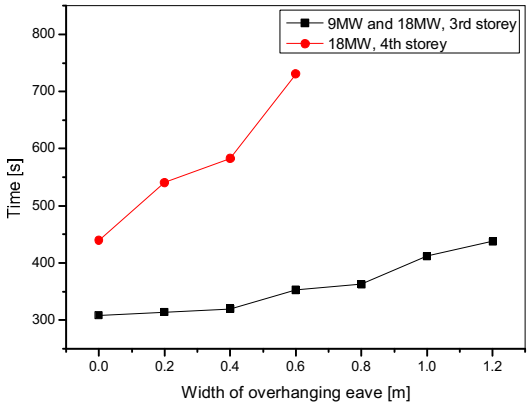

Fig.9. Time to reach 10kW/m^2 at the openings

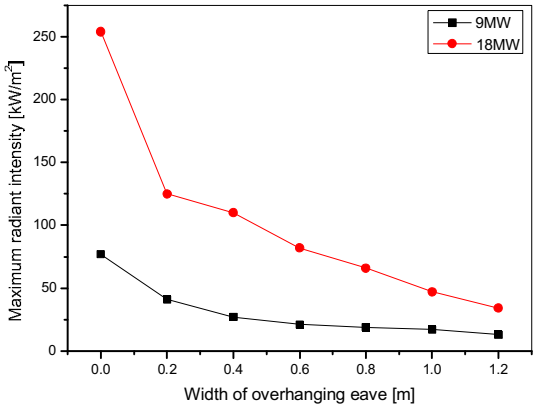

Fig.10. Maximum radiant intensity at the middle opening of the 3rd storey

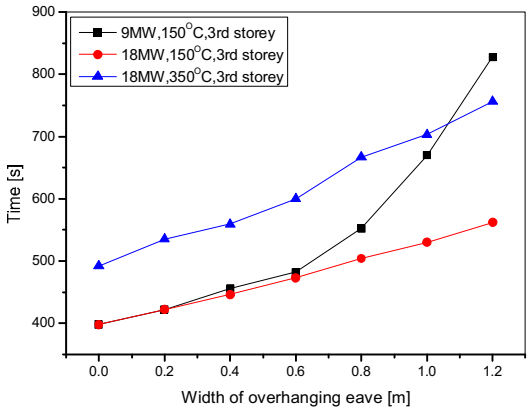

Fig.11 Time to reach 150℃ or 350℃ at the windows

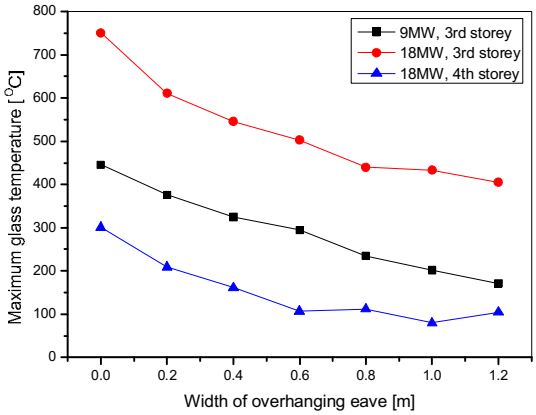

Fig.12. Maximum glass temperature at the middle windows of the 3rd and 4th storey

Fig.11. and *Fig.12.* show that the simulation results of the overhanging eaves at different widths with all windows close. With the overhanging eave, only the temperature at the middle windows of the 3rd storey could reach 150℃ for 9MW fire and reach 350℃ for 18MW fire. When the width of overhanging eave increased to 0.4m, the temperature at the middle windows of the 3rd storey was below 350℃. When the width of overhanging eave increased to 0.6m, the temperature at the middle windows of the 4th storey was below 150℃. *Fig.11.* shows that the time at which the temperatures on the exterior side of the windows reached to 150℃ and 350℃ increased with the increase of the width of overhanging eave. The maximum temperature at the middle window of the 3rd storey was decreased by an increase in width of the overhanging eave. However, the maximum temperature at the middle window of the 4th storey increased slightly when the width of overhanging eave increased from 1.0m to 1.2m. The reason was that too wide overhanging eave blocked the smoke movement and made the smoke get together under the overhanging eave. Then the temperature at the upper portion of the window increased.

3 CONCLUSIONS

CFD simulations were carried out to study the effects of wall pier and fire resistant overhanging eaves in preventing vertical fire spread. The fires at 9MW and 18MW were set to represent the typical office fire, hotel fire and shop fire. The simulation results show that increasing the height of wall pier has little effects on preventing vertical fire spread. There is an optimum height of wall pier for different fire scenarios. Excessive increasing the height of wall pier will induce the outside smoke and flame closer to the exterior wall and make the fire spread vertically easily. The fire resistant overhanging eave has a much better effect on preventing fire from spreading vertically than wall pier. Increasing the width of fire resistant overhanging eave will reduce vertical fire spread. However, too wide overhanging eave will obstruct the upward movement of the smoke and make more smoke flow into the room in the upper stories through the openings.

REFERENCES

[1] National Fire Protection Association. NFPA 5000: Building Construction and Safety Code, 2006.
[2] International Code Council, 2006 International Building Code, *ICC Inc*, 2005.
[3] Ministry of Construction of the P.R.China, GB 50016-2006: Code of Design on Building Fire Protection and Prevention, 2006.
[4] Ministry of Construction of the P.R.China, GB 50368-2005: Residential Building Code, 2005.
[5] Thomas J.O., George W.M., Fire Tests of Single Office Workstations, *National Institute of Standards and Technology Report NIST-NCSTAR-1-5C*, 2005.
[6] National Institute of Standards and Technology, Sofa Fire, *http://www.fire.nist.gov/fire/fires/sofa/*
[7] Tianjin Fire Research Institute, Fire Risk Analysis and Assessment, *Research Report of 10th five-year plan of China*, 2004.
[8] National Fire Protection Association. NFPA 92B: Guide for Smoke Management Systems in Malls, Atria, and Large Areas, 2000.
[9] Standards New Zealand, SNZ PAS 4509: New Zealand Fire Service Fire Fighting Water Supplies Code of Practice, 2003.
[10] Bukowski, R.W., Clarke, F.B., Fire Risk Assessment Method: Description of Methodology, *National Fire Protection Research Foundation*, 1990.
[11] Hadjisophocleous, G.V., Benichou, N., and Tamim, A.S., Literature Review of Performance-Based Fire Codes and Design Environment, *Journal of Fire Protection Engineering*, 9(1): 12-40.

DECREASE IN FIRE LOAD ON STRUCTURES BY TIMELY FIRE DETECTION

Aleš Dudáček [a]

[a] VŠB – Technical University of Ostrava, Faculty of Safety Engineering, Ostrava, Czech Republic

INTRODUCTION

One way of increasing fire safety in buildings is the use of fire safety devices (henceforth referred to as FSD). The basic division of them is presented in Decree No. 246/2001 Coll. of Ministry of the Interior. The fire safety devices that are of key importance to an increase in fire safety are listed in Section 4 of the above-mentioned Decree and are designated as reserved kinds of fire safety devices. Depending upon function and purpose, some reserved fire safety devices influence directly the course of a fire (e.g. fixed fire fighting systems) and can be used, in the framework of dealing with fire safety in buildings, for fire risk reduction. However, in a case of the devices that do not have any direct influence on the course of a fire, the installation of these devices cannot lead to fire risk reduction. But the use of such devices can be a condition for including another fire risk reducing coefficient into calculations (e.g. the use of fire detection and alarm system (FDAS) is a condition for including the reducing coefficient for fire brigade intervention into calculations). Timely fire detection and alarm are also of great importance to the evacuation of persons, and shortening the time to evacuation thanks to the timely raising of the alarm by the FDA system makes it possible, e.g. to extend unprotected escape routes. The fast intervention of fire brigades, the use of fixed fire fighting systems and smoke and heat exhaustion systems have direct effects on the course of a fire in space, and thus also on thermal load on structures. The obvious condition is the reliable function of fire safety devices and their correct design and installation. In the text below the analysis of function of fire detection and alarm system (FDAS), fixed fire fighting system (FFS) and smoke and heat exhaustion system (SHES) in the course of fires in the Czech Republic in the years 2006 and 2007 will be provided and the influence of SHES on the course of a fire will be shown by means of software for fire modelling.

1 ANALYSIS OF THE FUNCTION OF SELECTED FIRE SAFETY DEVICES IN THE COURSE OF FIRES IN THE CZECH REPUBLIC

The Ministry of the Interior – General Directorate of Fire and Rescue Service of the Czech Republic keeps the national statistics on fires and other incidents (Statistical Observation of Events – SOE) [2], in which fire brigades intervened. This statistical observation of events provides valuable data for the analysis of fires, the causes of fires and the courses of fires, and can also be used for the analysis of function of selected fire safety devices during the fires.
The main objective of use of FDASs is shortening the time to fire discovery, notification and acceptance of other needed measures. On the basis of data from SOE in the period from 1997 to 2003, a comparison between the time to fire discovery and the time to fire notification to the emergency call centre in the case of correct function of FDAS and without the influence of FDAS on these times was carried out [1]. The influence of automatic fire detection on the shortening of the time to fire discovery in buildings, which is taken into account when considering fire alarm application, i.e. buildings of classes 1, 2, and 3 from the point of view of ID, can help us to get a better picture. On the basis of data on times to fire discovery and receiving the emergency call, distribution functions of times to discovery (Fig. 1) and to

receiving the emergency call (Fig. 2) in cases without FDAS influence and in cases, when FDAS fulfilled its function in fire detection were created for these classes of buildings. The FDAS influence on the increase in the number of fires discovered, or reported shortly after their origin is clear from Figs. 1 and 2.

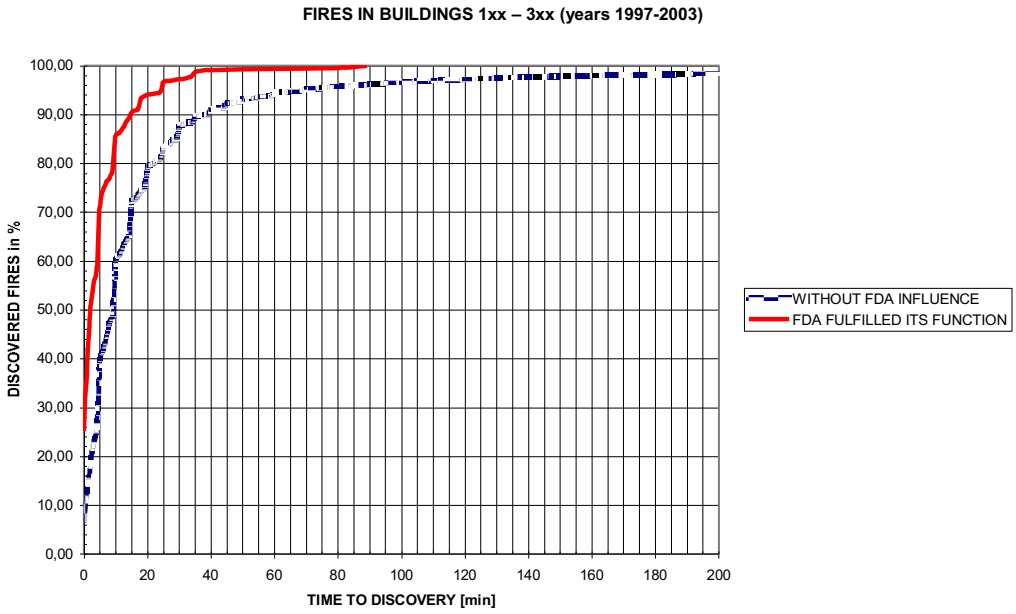

Fig. 1. Distribution functions of times to discovery

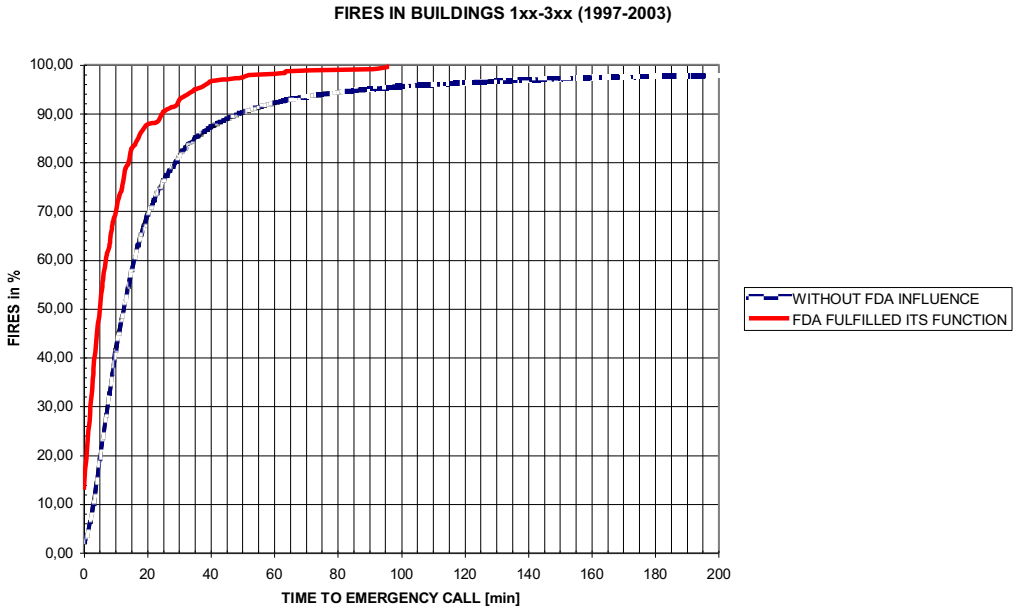

Fig. 2. Distribution functions of times to receiving the emergency call

1.1 Overview of Fires in the Years 2006 and 2007

On the basis of statistical data on SOE, the analysis of function of fire detection and alarm system (FDAS), fixed fire fighting system (FFS), combustible gas and vapour detection system (CGVDS) and smoke and heat exhaustion system (SHES) during the fires in the Czech Republic in the years 2006 and 2007 was made. For the analysis, only fires in buildings relevant for the use of mentioned fire safety devices were considered; according to the SOE code-list, it was the case of buildings of 1xx, 2xx, 3xx, 4xx, 530, 531, 550, 552, 554, 555, 556, 557 and 992 classes. A basic overview of fires in the given buildings in the years 2006 and 2007 is presented in Table 1.

Table 1. Overview of selected fires in the years 2006 - 2007

	YEAR	
	2006	2007
Total number of fires in the Czech Republic	20 540	22 394
Number of fires in buildings of selected classes	5 491	5 532
Number of members of Integrated Emergency System killed in selected fires	0	0
Number of members of Integrated Emergency System injured in selected fires	116	110
Number of persons killed in selected fires	86	60
Number of persons injured in selected fires	471	542
Number of persons rescued from selected fires	352	409
Number of persons evacuated in the course of selected fires	3 082	3 055

Thus, approximately one quarter of all the fires (26.7% in 2006 and 24.7% in 2007) in the years 2006 and 2007 occurred in buildings relevant to the use of selected fire safety devices; nevertheless, the proportions of killed and injured persons in the total number were markedly higher.

1.2 Function of Selected FSDs in the course of Fires

As for fires in buildings of the above-mentioned selected classes, the function of FDAS, FFS, CGVDS and SHES was observed. For clarification, the function of each system was merely divided into two categories – the device fulfilled the task or the device did not fulfil the task in the fire, although it had been installed in the building. Into the category, when FSD did not fulfil the task in the fire, cases of installations of the device outside the space of fire origin, cases of device failure, device switching off and cases when the functional device did not respond to the fire (also the release of combustible gases and vapours) were included. An overall overview of function of selected FSDs in the fires is provided in Fig. 3. From the figure, it is evident that only in FDASs, the proportion of cases when the system fulfilled the task is markedly higher than the proportion of cases when the system did not fulfil the task in the fire. In the other FSDs, differences are not obvious so much; in FFSs and SHESs, cases when the device did not fulfil the task in the fire prevailed in both the years. Here it is necessary to state that the most frequent cause for the not fulfilment of the task in the fire was the installation of the device outside the space of fire origin. Non-functionality in the fire was found out in five EDASs, four FFSs and three SHESs. In one case, technically functional FDAS and also in one case, technically functional FFS did not respond to fire origin. On the basis of Fig. 3, it is also possible to state that in the year 2007, in the case of all selected FSDs the FDS number in fire-affected buildings was reduced. This should be evaluated, with regard to the positive influence of FSDs on the reduction of fires and fire consequences, negatively.

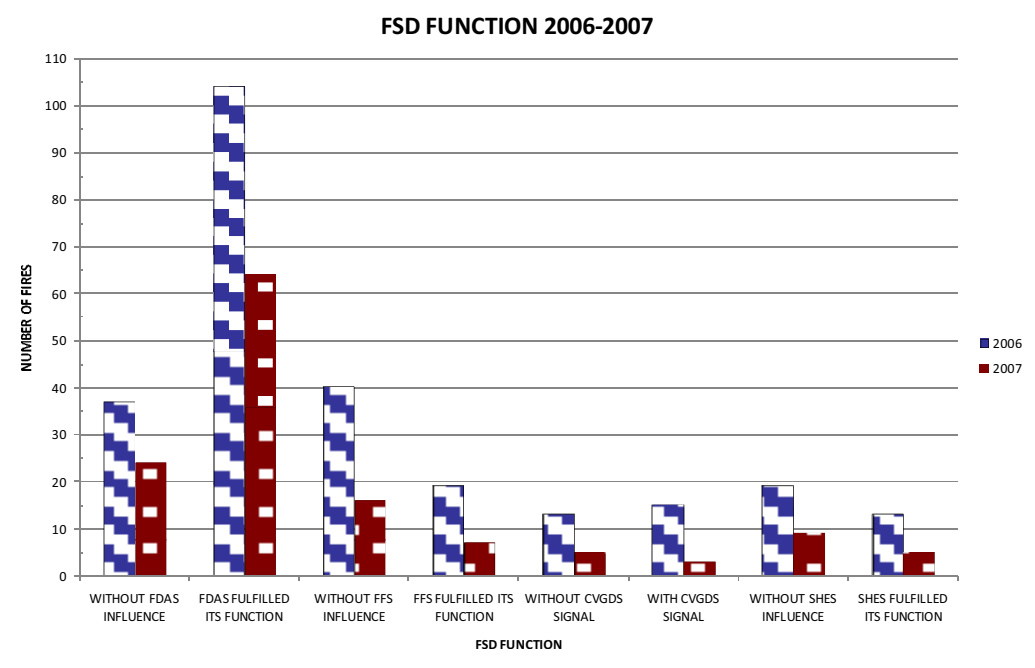

Fig. 3. Overview of the function of selected FSDs in the fires

2 INFLUENCE OF SOME FSD'S ON THE COURSE OF A FIRE

As already stated in Introduction, some fire safety devices influence directly the course of the fire, and it is possible to use them for influencing the fire risk when designing fire safety in buildings. For the purposes of evaluation of their influence, the mathematical modelling of the course of the fire by means of an ARGOS zone model was used. Software ARGOS is a product of Danish Institute of Fire and Security Technology (DIFT) from Copenhagen; at present, version 5.3 is used. The CFD models (e.g. FDS program developed at the National Institute of Standards and Technology (NIST) – Building and Fire Research Laboratory in Gaithersbursburg, U.S.A.) provide, in a number of cases, more accurate results; on the other hand, they are more computationally intensive. An advantage of FDS program is also the fact that results can be graphically plotted by means of Smokeview software.

For calculations, a dummy single-storeyed hall for wood processing of the floor size 12 m x 18 m and the height of 5 m. was used. The structure of the building is reinforced concrete. For the considered fire load p_n of 60 kg.m^{-2}, the fire safety level II is required for the building according to the new draft standard ČSN 73 0802. In the hall, automatic fire alarms with temperature and smoke detectors were used; the temperature ones having the value (temperature) of response of 70 °C and the response time index RTI = 300 (m.s)$^{1/2}$, the smoke ones with the sensitivity of 0.30 dB.m^{-1}. If SHES was considered in the calculations, it was a case of natural exhaustion of smoke and heat triggered by a thermal fuse with the reaction temperature of 70 °C and the response time index RTI = 100 (m.s)$^{1/2}$. The aerodynamic area of SHES, which was determined on the basis of SHES hole area with using the discharge coefficient c_v = 0.60, is presented in Table 3. The time delay in opening (proper opening time) was set at 10 sec. The hall was connected with the surrounding environment by means of two doors, two gates and altogether three holes. The size, opening and closing of them in the

course of individual tests are given in Table 3. For the calculations, four variants of initial fires were used; they were variants of stacked Euro pallets. The basic description of them is presented in Table 2. For each variant of initial fire, six calculations under various conditions were executed. Altogether, 24 fire scenarios were dealt with.

Table 2. Initial fires used

	Initial fire			
	A	B	C	D
Height of pallets [m]	1.0	1.5	1.7	2.0
Width of pallets [m]	0.8	1.6	1.6	1.6
Length of pallets [m]	6.0	6.0	6.0	6.0
Volume of pallets [m^3]	4.80	14.40	16.32	19.20
Heat release rate [MW]	16.80	50.40	57.12	67.20
Total energy released [MJ]	16 130	48 400	54 800	64 500

Table 3. Conditions used in calculation – fire scenarios

	Number	Fire scenario					
		1	2	3	4	5	6
Door 140 x 210 cm	2	Close	Close	Close	Close	Close	Close
Gate 300 x 300 cm	2	Close	Close	Close	Close	Close	Close
Hole 50 x 50 cm, 200 cm above the floor	1	Open	Open	Open	Open	Open	Open
Hole 300 x 300 cm	1	Close	Open	Open	Open	Open	Open
Hole 300 x 300 cm	1	Close	Close	Close	Close	Close	Open
SHES aerodynamic area [m^2]	1	N/A	N/A	2.16	4.32	6.50	6.50

Table 4. Time of occurrence of Flash-over phenomenon according to fire scenarios

Occurrence of Flash-over phenomenon [mm:ss]	Fire scenario					
Type of initial fire	1	2	3	4	5	6
A	No	No	No	No	No	No
B	09:45	No	No	No	No	No
C	08:45	09:55	10:35	No	No	No
D	07:36	08:35	09:05	09:25	09:55	No

From Table 4 it is evident that smaller aerodynamic areas of SHES were not sufficient to prevent the Flash-over phenomenon. If in the case of scenario B2, natural ventilation through a 3 m x 3 m hole in the wall was sufficient to prevent the Flash-over, then in the case of scenario D5, SHES with the aerodynamic area, which corresponded to 3% of floor area, did not prevent the Flash-over. The reason was the insufficient supply of air into the ventilated compartment (open area of 9 m^2). If this area was doubled (scenario D6), the Flesh-over did not occur any more.
Basic data on the course of the fire according to some selected scenarios are presented in Table 5.

Table 5. Course of the fire according to some selected scenarios

	Fire scenario						
	A1	B1	B2	C3	C4	D5	D6
Flash-over [min:sec]	N/A	09:45	N/A	10:35	N/A	09:55	N/A
Temperature detector response [min:sec]	03:25	03:01	03:01	02:57	02:57	02:54	02:54
Smoke detector response [min:sec]	01:10	01:10	01:10	01:10	01:10	01:10	01:10
SHES opening [min:sec]	N/A	N/A	N/A	02:32	02:32	02:32	02:32
Maximum temperature of upper layer [°C]	222	1 123	461	1 160	462	1 178	458

In Table 5 the great difference in the achieved temperature of upper layer between the case when the Flash-over occurs and the case when it does not occur can be seen. It is possible to demonstrate this difference on an example of scenarios D5 and D6; curves of upper layer temperatures are there in Figs. 4. and Fig. 5.

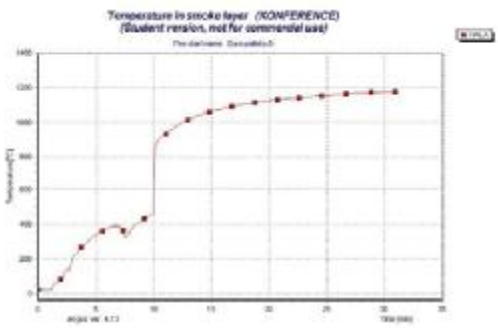

Fig. 4. Upper layer temperature, D5

Fig. 5. Upper layer temperature, D6

To complete the view of theoretical temperatures of the fire, comparison with the standard temperature curve according to ČSN EN 1363-1 (also according to ISO 834:1975) or, as the case may be, with the hydrocarbon temperature curve according to ČSN EN 1363-2 is possible.

3 SUMMARY AND ACKNOWLEDGMENT

The made analysis of fire statistics shows clearly the importance of use of automatic fire detection to shorten the time to fire notification, and thus to fire brigade intervention. By ARGOS software, the impact of SHES application on Flash-over phenomenon prevention was calculated. The prevention of Flash-over leads unambiguously to markedly lower temperatures in the fire, and thus to the limitation of damage to structures as well as internal equipment. The calculation confirms the expected faster response of smoke fire detector in comparison with the temperature detector.

REFERENCES

[1] Dudáček, Aleš – Stryková, Zuzana. Problematika používání automatických hlásičů požáru v budovách pro bydlení a ubytování. In *Zborník Wood & Fire Safety 2004*. Zvolen: TU Zvolen, 2004. pp. 35 – 44.

[2] Statistické sledování událostí. Praha: GŘ HZS ČR, 2008.

ADIABATIC SURFACE TEMPERATURE
A Sufficient Input Data for a Thermal Model

Joakim Sandström [a], Ulf Wickström [b], Milan Veljkovic [c]

[a] Luleå University of Technology/Brandskyddslaget AB, Karlstad, Sweden
[b] Luleå University of Technology/SP Technical Research Institute of Sweden, Borås, Sweden
[c] Luleå University of Technology, Luleå, Sweden

INTRODUCTION

Two computational models are employed in this paper to predict structural performance in fire:

- A fire model created using a numerical code based on Computation Fluid Dynamic (CFD). The model predicts the development of a fire and the heat flux in a fire compartment with a simple geometry consisting of solid objects for the purpose of estimating their temperature.
- A thermal/structural model using numerical software based on the Finite Element Method. The model predicts structural behaviour based on an "effective gas temperature", which is denoted *adiabatic surface temperature*. This temperature may be obtained either from fire modelling or from measurements. An important question is which parameter values from the fire model are required to transfer information at the gas-solid interface.

A thorough and common understanding of heat transfer to structural elements of a building is very important for realistic prediction of the temperature and resistance of structural components. Researchers and test standard developers have different ways of expressing and measuring the various forms of convective and radiative heat flux.

The net heat flux to a surface computed by a fire model is often seen as a valuable information to be used in thermal/structural model to perform detailed heat transfer calculation within the structural elements. However the net heat flux calculated in the fire model depends on the corresponding surface temperature and is therefore limited to be used in thermal calculations only with the same structural geometry as used in the fire model.

This paper is intended to promote use of *adiabatic surface temperature (AST)* [1] as a practical means of expressing the thermal exposure of structural surfaces independent of the structural properties in the fire model. The concept is useful when calculating temperatures and structural resistance in a fire.

The concept of AST may be used when the exposure conditions are obtained either from a fire model, calculated by the Fire Dynamic Simulator, FDS [2] or directly from measurements using Plate Thermometer temperatures [3].

1 THEORETICAL BACKGROUND OF HEAT TRANSFER

Heat is transferred from hot fire gases to structures by radiation and convection. The contributions of these two models of heat transfer are in principal independent and must be treated separately.

Thus the total heat flux $\dot{q}''_{tot}$ to a surface is:

$$\dot{q}''_{tot} = \dot{q}''_{rad} + \dot{q}''_{con} \tag{1}$$

where $\dot{q}''_{rad}$ is the net radiation heat flux and $\dot{q}''_{con}$ the heat transfer to the surface by convection. The net contribution by radiation $\dot{q}''_{rad}$ depends on the incident radiation $\dot{q}''_{inc}$, on the surface emissivity/absorptivity, Stefan-Boltzmanns constant, σ, and on the fourth power of the absolute temperature T_s of the targeted surface. The heat exchange at a surface is illustrated by *Fig. 1*.

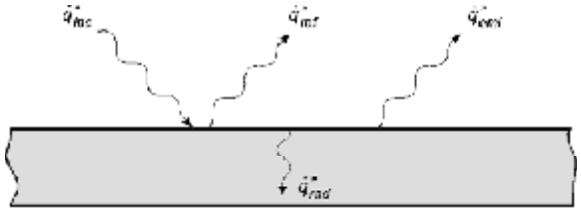

Fig. 1 The heat transfer by radiation to a surface depends on incident radiation and the surface absolute temperature and the surface emissivity.

A part of the incident radiation is absorbed and the rest $\dot{q}''_{ref}$ is reflected. Then the surface emits heat by radiation $\dot{q}''_{emi}$ depending of the emissivity and the surface absolute temperature to the fourth power. Thus

$$\dot{q}''_{\mathrm{rad}} = \alpha_{\mathrm{s}}\dot{q}''_{\mathrm{inc}} - \varepsilon_{\mathrm{s}}\sigma T_{\mathrm{s}}^4 \tag{2}$$

where α_{s} and ε_{s} are the target surface absorptivity and emissivity, respectively. The surface emissivity and absorptivity are assumed equal according to the Kirchhoff's identity, and the incident radiation is expressed in terms of a radiation temperature, T_{r}. Then (2) becomes:

$$\dot{q}''_{\mathrm{rad}} = \varepsilon_{\mathrm{s}}\sigma(T_{\mathrm{r}}^4 - T_{\mathrm{s}}^4) \tag{3}$$

The heat transferred by convection from adjacent gases to a surface varies a lot depending on adjacent gas velocities and geometries. It may be written as

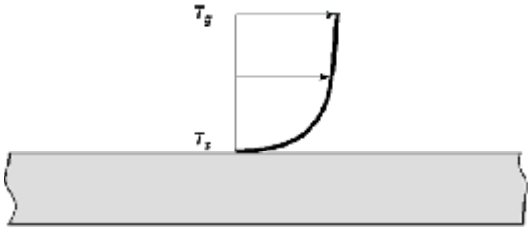

Fig. 2 Gas velocity profile. The heat transfer by convection depends on the temperature difference between the adjacent gases and the target surface, and on the gas velocity.

$$\dot{q}''_{\text{con}} = h(T_{\text{g}} - T_{\text{s}}) \tag{4}$$

The convective heat transfer coefficient *h* depends mainly on flow conditions near the surface and not so much on the surface or the material properties.
The total heat transfer to a surface may now be obtained by adding the contributions by radiation and convection:

$$\dot{q}''_{tot} = \varepsilon_s \sigma (T_r^4 - T_s^4) + h(T_g - T_s) \tag{5}$$

1.1 Adiabatic Surface Temperature (AST)

The two boundary temperatures in (5), T_{r} and T_{g} may be combined to one effective temperature T_{AST}, the adiabatic surface temperature. This temperature is defined as the temperature of an ideally perfectly insulated surface when exposed to radiation and convection heat transfer [1]. Thus T_{AST} is defined by the surface heat balance equation

$$\varepsilon_s \sigma (T_r^4 - T_{AST}^4) + h(T_g - T_{AST}) = 0 \tag{6}$$

The value of T_{AST} is always between T_{r} and T_{g}.
By combining (5) and (6) the total heat transfer may be written as

$$\dot{q}''_{\text{tot}} = \varepsilon_{\text{s}} \sigma (T_{\text{AST}}^4 - T_{\text{s}}^4) + h(T_{\text{AST}} - T_{\text{s}}) \tag{7}$$

2. PRACTICAL APPLICATION OF AST

Three components are assumed or calculated in thermal response of fire exposed structures. The first component and the most common to assume is the time-temperature curve, or fire temperature based on the assumed surrounding conditions, used to heat the structural element. The second and third is the heat flux and surface temperature which are calculated based on the properties of the structural element.

FDS can calculate the fire progression for a desired scenario and with a 1-D heat flow model calculate the second and third components of the thermal response calculation. These values are only valid for the structural properties used in the FDS calculation but can be seen as fairly accurate [4].

By knowing the surface temperature, T_s and the heat flux from radiation, $\dot{q}''_{rad}$ and convection, $\dot{q}''_{con}$ FDS can use equation 6 to iteratively calculate the assumed fire temperature in each time step [5] representing the surrounding temperature and therefore valid for any structural element. This fire temperature calculated in FDS is denoted T_{AST}.

By specifying T_{AST} as an output in FDS it is possible to obtain a time-temperature curve in each direction of fire exposure of a structural element that is calculated for the specific

scenario used in the fire model. This time-temperature curve can be used in thermal FEM-calculations the same way as fire curves such as the ISO834 or ASTM 119-E with the difference that there are different values for each side whereas the temperature exposure of ISO834 and ASTM 119-E are uniform.

2.1 Numerical example

To show that, by knowing T_s and $\dot{q}''_{tot}$, it is possible to derive a fire curve with T_{AST} that is valid for other structural elements than the one used in the first calculation. Two different fire simulations were performed in a room of the dimension 1.6 m by 1.6 m and 1.6 m high with a steel beam (tubular cross section) in the ceiling. An opening of 1.2 m by 0.8 m was modelled at the wall opposite of a heat source, see Fig. 3.

The heat source in the fire model was 0.2 m by 0.2 m with a constant heat release of 500 kW. Grid cells of 2.5 cm. The simulations were performed with different beam sizes: RHS 300 (300 mm by 200 mm with a thickness of 9.5 mm) and RHS 200 (200 mm by 100 mm with a thickness of 10.5 mm). T_{AST} was calculated in both cases, on each side of the beam and in the concrete at three reference cross-sections of the beam, positions indicated in Fig 4.

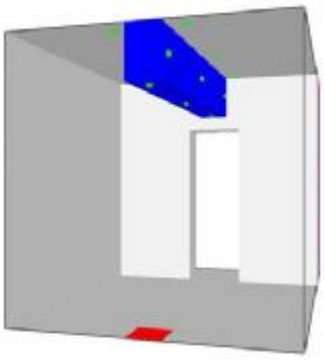

Fig. 3 The room used to model different scenarios. The red rectangle symbolizes the heat source.

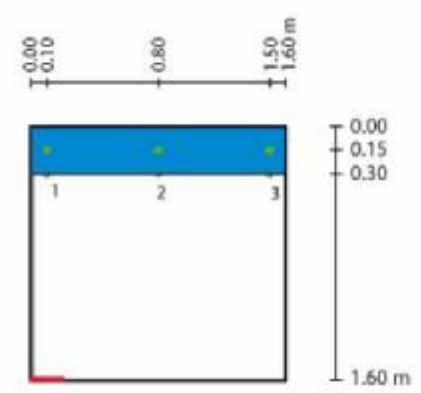

Fig. 4 Position of reference cross-sections at the steel beam.

The temperature distributions in the steel beams were calculated using Tasef [6]. T_{AST} from the corresponding reference points obtained from the fire model (FDS analyses) in each reference cross-section were the only boundary conditions used in the thermo-model, see Fig. 5. Different boundary conditions were assumed on each side of the beam (see fig 6.). The set up of the Tasef model is shown in fig 7.

Following assumptions were made to simplify the steel temperature calculations in Tasef:

- The model is symmetric around y-axis.
- Nodes in the steel section close to each other are coupled (restricted to get the same temperature) to save computational time.
- Heat transfer by radiation and convection inside the beam is considered.

All surfaces have an emission coefficient of 0.8 and the convection heat transfer coefficient $h = 25\ \mathrm{W/(m^2 K)}$.

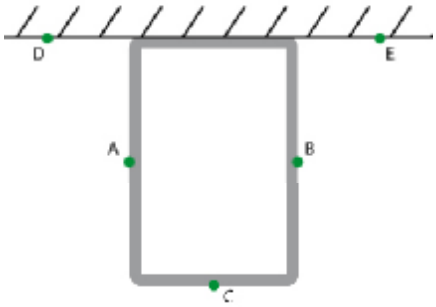

Fig. 5 Reference points in the fire model at the cross section of the beam in which the time-T_{AST} relations were calculated.

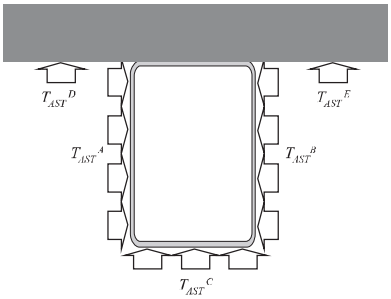

Fig. 6 The surfaces in the thermal model were exposed to the time-temperture cure with T_{AST} obtained from the corresponding surface in the fire model.

By assuming that:

- T_{AST} can be used in thermal calculations with good results [4]
- T_{AST} is valid for other structural elements than the one used in the fire model.

a comparison was made between thermal calculations on the larger beam (RHS 300) with T_{AST} from each of the fire simulations.

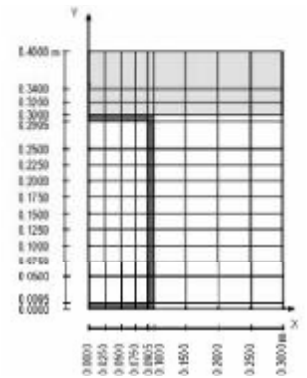

Fig 7. 2D thermo-model used in the Tasef calculations.

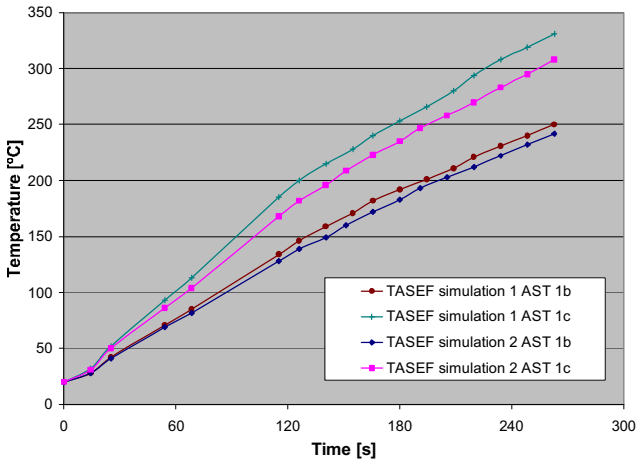

Fig. 8 Comparison of the temperature calculations performed in Tasef with the use of T_{AST} from two different FDS-calculations. T_{AST} taken as output from cross-section 1 and used as input in reference points b and c.

The results of the calculations are shown in Fig. 8 to show the influence of T_{AST} obtained in the two fire models. Temperature evaluation at the section 1 of the steel beam, in the middle of the bottom flange and in the web, points c and b, respectively are shown

One can conclude from Fig. 8 that it is possible to use T_{AST} obtained from the fire model with different beam sections as input for the thermo model. The shape of the curves are rather similar, but of course, differences exist for the various reference points due to the fact that geometry is a factor in the near field as in the case.

3 SUMMARY AND RECOMMENDATION FOR FURTHER WORK

The general idea of using the concept of adiabatic surface temperature T_{AST} in modelling heat transfer to fire exposed structures is illustrated in the paper. This is an initial part of the research planned to be performed at LTU.

The uncertainties introduced by employing T_{AST} are most often negligible as it has been shown in ref. [4]. There is a need to better understand, and allow compensation for, these uncertainties. After that it will be possible to perform thermal calculations in structural elements exposed to fire with the improved accuracy and flexibility needed in a new generation of the design process.

REFERENCES

[1] Wickström, U., (2007). Methods for Predicting Temperature in Fire Exposed Structures, *SP Draft*, SP - Swedish National Testing and Research Institute, Borås, 2007

[2] McGrattan, K.B., Hostikka S., J.E. Floyd, H.R. Baum and R.G. Rehm, Fire Dynamics Simulator (Version 5), Technical Reference Guide, *NIST SP 1018-5*, National Institute of Standards and Technology, Gaithersburg, Maryland, December 2008

[3] Wickström, U., Heat Transfer and Temperature Calculations Based on Plate Thermometer Measurements, *SP Draft*, SP - Swedish National Testing and Research Institute, Borås, 2008

[4] Wickström,U., Duthinh, D. and McGrattan, K.B., Adiabatic Surface Temperature for Calculating Heat Transfer to Fire Exposed Structures, *Interflam* 2007

[5] McGrattan, K., Hostikka S., Floyd, J., Klein, B., Fire Dynamics Simulator (Version 5), User's Manual, *NIST SP 1019-5*, National Institute of Standards and Technology, Gaithersburg, Maryland, December 2008

[6] Sterner, E. and Wickström, U., TASEF - Temperature Analysis of Structures Exposed to Fire, *SP Report 1990:05*, Swedish National Testing and Research Institute, Borås, 1990

[7] EN 1991-1-2, Eurocode 1: Actions on structures – Part 1-2: General actions – Actions on structures exposed to fire